TU WIEN

TECHNISCHE
UNIVERSITÄT
WIEN
Vienna | Austria

Diploma Thesis

Analysis of 24h Mobil-O-Graph pulse wave analysis measurements in a normative population cohort

Carried out at the

Institute of Electrodynamics, Microwave and Circuit Engineering

TU Wien

supervised by

Univ.Lektor Dipl.-Ing. Dr.techn. Bernhard Hametner,
Univ.Lektor Dipl.-Ing. Dr.techn. Christopher Mayer,
and Ao.Univ.Prof. Dipl.-Ing. Dr.techn. Eugenijus Kaniusas

by

Johannes Weber

Garbergasse 11/21
A-1060 Vienna

Vienna, September 27, 2016

Statutory Declaration

I declare that I have authored this thesis independently, that I have not used other than the declared sources/resources, and that I have explicitly marked all material which has been quoted either literally or by content from the used sources.

Vienna, _____   _____

　　　　　　　　Date　　　　　　　　　　　　　　　Signature

Eidesstattliche Erklärung

Ich erkläre an Eides statt, dass ich die vorliegende Arbeit selbstständig verfasst, andere als die angegebenen Quellen/Hilfsmittel nicht benutzt, und die den benutzten Quellen wörtlich und inhaltlich entnommenen Stellen als solche kenntlich gemacht habe.

Wien, am _____   _____

　　　　　　　　Datum　　　　　　　　　　　　　　Unterschrift

Acknowledgement

Abstract

Cardiovascular diseases (CVD) are the number one cause of death worldwide. Hemodynamics describes the fluid dynamics of the blood flow in the cardiovascular system (CVS). There are many different parameters coming from hemodynamics describing the health status of the CVS. In order to earlier and better detect CVDs a new approach is on its way to be established. The well-known ambulatory blood pressure monitoring (ABPM) is combined with pulse wave analysis (PWA). ABPM means recording blood pressure (BP) parameters at regular intervals with an automated device for example over 24 hours. PWA is used to determine the parameters near the heart termed as central or aortic parameters, in contrast to the common peripheral measurements at the upper or lower arm. The aim of this diploma thesis is to contribute to the task of establishing normal values for 24-hour measurements of central hemodynamic parameters, as well as showing an approach for the data evaluation and graphical representation.

In Luebeck, Germany, a healthy population cohort consisting of 93 experimentees was recruited. They were advised to wear an automated ambulatory blood pressure monitor for 24 hours. The device used in this study was the Mobil-O-Graph from I.E.M. GmbH, Stolberg, Germany. The Mobil-O-Graph is the first device which combines PWA and ABPM. Thus, additionally to the common 24-hour assessment of peripheral blood pressure, central hemodynamic parameters can be evaluated over 24 hours as well.

The data is classified by age, sex, and into day and night intervals. For the data evaluation the mean values of the groups are calculated and with statistical analysis the groups are analysed for differences. The graphical representation consists of 24-hour plots, where the data is smoothed before, and day/night scatter plots over age.

The main findings of this thesis are the lower heart rate of men compared to women but the blood pressure parameters are higher of women than of men. The reflection magnitude, augmentation pressure, augmentation index, and augmentation index at $75\,\text{min}^{-1}$ are higher for women than for men. The heart rate, peripheral and central systolic and diastolic BP values, and augmentation index at $75\,\text{min}^{-1}$ are higher during day compared to the night. The reflection magnitude, augmentation pressure, and augmentation index are elevated during the night. A close positive correlation was found between age and pulse wave velocity. There is a strong negative correlation with age of the pulse pressure amplification for the day, but no correlation for the night interval. The reflection magnitude, augmentation pressure, and augmentation index have a high correlation coefficient during the day as well as for the night. The age groups differ most significantly for the pulse wave velocity. The pulse pressure amplification decreases over age, the reflection magnitude, augmentation pressure, augmentation index, and augmentation index at $75\,\text{min}^{-1}$ increase with age.

In this thesis one approach is shown for the data evaluation and graphical representation of 24-hour hemodynamic parameters. Nevertheless, still a lot of work has to be done to identify hemodynamic parameters as marker for cardiovascular diseases, as well as to establish characteristic values.

Kurzfassung

Die Todesursache Nummer 1 weltweit sind kardiovaskuläre Erkrankungen. Die Hämodynamik ist die Strömungslehre über den Blutfluss im kardiovaskulären System aus der verschiedene Parameter hervorgehen, um den Gesundheitszustand des kardiovaskulären Systems zu beschreiben. Um Parameter und Methoden zu erhalten, die zu aussagekräftigeren Parametern führen, gibt es einen neuen Ansatz. Ambulantes Blutdruck-Monitoring wird mit Pulswellenanalyse kombiniert. Ambulantes Blutdruck-Monitoring ist das Aufzeichnen von Blutdruckparameter in regelmäßigen Intervallen mit einem automatisierten Gerät über zum Beispiel 24 Stunden. Pulswellenanalyse erlaubt es hämodynamische Parameter nahe beim Herzen zu ermitteln, im Gegensatz zu den üblichen peripheren Werten, die am Ober- oder Unterarm ermittelt werden. Diese werden dann als zentrale Parameter bezeichnet. Das Ziel dieser Arbeit ist es einen Beitrag zu leisten, um Normalwerte für 24-Stunden Messungen von zentralen Parametern zu etablieren. Des weiteren soll eine Methode aufgezeigt werden, wie die Daten ausgewertet und grafisch repräsentiert werden können.

In Lübeck, Deutschland, wurde eine gesunde Kohorte bestehend aus 93 Probanden rekrutiert. Diese wurden angewiesen, 24 Stunden einen automatisierten ambulatorischen Blutdruckmonitor zu tragen. Bei dem verwendeten Gerät handelt es sich um den Mobil-O-Graph von I.E.M. GmbH in Stolberg, Deutschland. Dies ist das erste Gerät, welches Pulswellenanalyse und 24-Stunden ambulatorische Blutdruckmessung vereint. Dies bedeutet, dass zusätzlich zu der 24-Stunden Aufzeichnung von peripheren Blutdruck, die zentralen hämodynamischen Parameter ebenso über 24 Stunden gemessen werden können.

Die Daten wurden nach Geschlecht, Alter und in Tag- und Nachtintervalle klassifiziert. Mittels statistischer Analysen werden die Parameter auf Unterschiede untersucht. Die grafische Repräsentation erfolgt mittels 24-Stunden Plots, wobei die Daten geglättet werden, und mit Scatterplots für die Tag/Nacht Intervalle.

Männer haben eine niedrigere Herzrate und höhere Blutdruckparameter verglichen mit Frauen. Die Reflexionsmagnitude, Augmentationsdruck, Augmentationsindex und Augmentationsindex @ 75 bpm sind bei Frauen höher als bei Männer. Herzfrequenz, periphere und zentral Blutdrücke, systolisch wie diastolisch, sowie der Augmentationsindex @ 75 bpm sind während des Tages höher als in der Nacht. Die Reflexionsmagnitude, Augmentationsdruck und Augmentationsindex sind in der Nacht erhöht. Eine starke positive Korrelation wurde zwischen dem Alter und der Pulswellengeschwindigkeit festgestellt. Eine stark negative Korrelation zeigt sich für die Pulsdruckamplifikation während des Tages, wobei sich in der Nacht keine Korrelation zeigt. Die Reflexionsmagnitude, Augmentationsdruck und Augmentationsindex haben eine hohe Korrelation während des Tages sowie nachts. In der Pulswellengeschwindigkeit unterscheiden sich die Altersgruppen am stärksten. Die Pulsdruckamplifikation sinkt mit dem Alter, die Reflexionsmagnitude, Augmentationsdruck, Augmentationsindex und Augmentationsindex @ 75 bpm steigen mit dem Alter.

In dieser Arbeit wird ein Ansatz gezeigt, wie man 24-Stunden Daten auswerten und graphisch repräsentieren kann. Es ist noch viel Arbeit, hämodynamische Parameter zu charakterisieren und Referenzwerte zu etablieren.

Contents

Symbols and Abbreviations

Note: Variables used within limited context are described at the relevant section and are not listed here.

ABPM   ambulatory blood pressure monitoring

AIx   augmentation index

AIx@75   augmentation index at $75\,\mathrm{min}^{-1}$

ANOVA   analysis of variance

AP   augmentation pressure

BMI   body mass index

BP   blood pressure

cDBP   central diastolic blood pressure

CI   confidence interval

CO   cardiac output

CO$_2$ carbon dioxide

cPP   central pulse pressure

cSBP   central systolic blood pressure

CV   cardiovascular

CVD   cardiovascular disease

CVS   cardiovascular system

DBP   diastolic blood pressure

ECG   electrocardiography

HR	heart rate
IQR	interquartile range
MAP	mean arterial pressure
NaN	Not a Number
P_b	backward pressure wave
pDBP	peripheral diastolic blood pressure
P_f	forward pressure wave
pMAP	peripheral mean arterial pressure
PP	pulse pressure
PPamp	pulse pressure amplification
pPP	peripheral pulse pressure
pSBP	peripheral systolic blood pressure
PWA	pulse wave analysis
PWV	pulse wave velocity
RM	reflection magnitude
SBP	systolic blood pressure
SV	stroke volume

Introduction

1.1 Motivation

Cardiovascular diseases (CVD) are the number one cause of death worldwide. In 2012, 17.5 million people died from CVDs, being $31\,\%$ of all deaths globally [53]. CVDs are pathologies of the cardiovascular system (CVS), hence, these are medical conditions of the heart, the blood vessels, and the blood. CVDs can be, among others, endothelial dysfunction, arteriosclerosis, aneurysm, hypertension, heart attack, tachycardia, and bradycardia [41]. There is a great interest in identifying pathologies of the CVS. The earlier a pathological condition is detected, the higher the chance of a successful medical treatment, or even better, adequate precautionary actions can be initiated.

Hemodynamics describes the fluid dynamics of the blood flow in the CVS. There are many parameters describing the health status of the CVS. Most popular and clinically used hemodynamic parameters are the heart rate, the systolic blood pressure, the diastolic blood pressure, and the mean arterial pressure. Blood pressure (BP) is usually measured at the upper arm with a blood pressure cuff. This BP, measured at the brachial artery, is commonly referred to as peripheral BP. Measurements are done in a doctor's office or at the hospital. Furthermore, a patient can do out-of-office measurements at home with an according blood pressure monitor.

Independently where and when the BP determination takes place, it is common to be a single measurement. BP is a dynamic value dependent from a lot of factors. There is consent that BP measured at only one point in time is not very reliable, but ambulatory blood pressure monitoring (ABPM) is more trustworthy. ABPM means to record the BP at regular intervals with an automated device, which allows repeated measurements for example over 24 hours. Thus, BP during daily activities and at night during sleep is recorded and can be evaluated. Hence, a better assessment of the parameter is possible. The patient wears a portable BP monitor including a cuff on the normally non-dominant arm and is advised to stand still and to put the arm with the cuff at heart level during the cuff inflation. [19]

Peripheral values are usually gained at the upper or lower arm. Hemodynamic parameters obtained at the aorta near to the heart are termed as aortic or central parameters. They are poten-

tially better in predicting cardiovascular (CV) events, when describing the CVS near the heart and the inner organs [44], like for example the pulse wave velocity [2] or the central systolic blood pressure [31, 21]. Invasive methods for obtaining central hemodynamic parameters are expensive and cumbersome for the patient. Pulse wave analysis (PWA) is a method which is on its way to become an established technique [55, 32]. After recording of the pulse wave a generalized transfer function is applied to this peripheral pulse wave to acquire the central pulse wave [34, 47, 46, 33, 5, 29, 7]. The central pulse wave is then analysed with PWA to determine the central hemodynamic parameters, which are, among others, the central systolic blood pressure, the central diastolic blood pressure, the central pulse pressure, the pulse pressure amplification, the augmentation index, the aortic pulse wave velocity, and the reflection magnitude. The recording of the pulse wave can be invasive as well as non-invasive.

The Mobil-O-Graph, an ambulatory PWA device, combines the two aspects of ABPM and PWA and records the pulse wave non-invasively at the upper arm. Thus, it is possible to record and assess central hemodynamic parameters over a certain time interval, which enables to investigate established as well as new parameters under a new perspective. A lot of work has been already done validating new devices and investigating central hemodynamic parameters and their ability to forecast CV events [2, 31, 26, 3, 11, 46, 51, 50, 21], but little work has been done analysing 24-hour recordings.

1.2   Aim of this work

The 24h monitoring of hemodynamic parameters is not yet clinically used. In order to change that a characterisation of hemodynamic parameters is necessary as well as establishing reference values. The aim of this thesis is to contribute to this task with the novel approach of 24-hour PWA recordings done with an entire healthy population. Another aim is to show an approach how the data evaluation and graphical representation can be done. The aim is not to contribute to determining pathologies with the use of hemodynamic parameters. The parameters which are evaluated in this work are the heart rate *HR*, peripheral diastolic blood pressure *pDBP*, peripheral systolic blood pressure *pSBP*, peripheral pulse pressure *pPP*, peripheral mean arterial pressure *pMAP*, central diastolic blood pressure *cDBP*, central systolic blood pressure *cSBP*, central pulse pressure *cPP*, pulse pressure amplification *PPamp*, augmentation index *AIx*, augmentation index at $75\,\mathrm{min}^{-1}$ *AIx@75*, augmentation pressure *AP*, reflection magnitude *RM*, forward pressure wave P_f, backward pressure wave P_b, and pulse wave velocity *PWV*.

The data material is analysed for sex differences, age dependencies, and temporal variation. This is done by classifying the data and executing statistical analysis, and via graphical representation of the classified data. Hence, a further aim is to implement MATLAB functions for the data evaluation and for plotting purposes.

1.3   Outline

This thesis is structured in six chapters. After this introduction, the chapter physiological background (2) describes the cardiovascular system (2.1) as well as the hemodynamic parameters (2.2) discussed in this work. The chapter data acquisition (3) describes the study design (3.1)

and the used device, the Mobil-O-Graph (3.2). Afterwards, the chapter methods (4) describes the methodology that has been used and implemented to obtain the results stated in chapter 5. The methods are divided into data preprocessing (4.1), data evaluation (4.2), and the graphical representation (4.3). The last chapter is a discussion of the results (chapter 6).

CHAPTER **2**

Physiological Background

2.1 Cardiovascular System

The cardiovascular system (CVS) (also called circulatory system) is an enclosed system where the blood circulates across the body. It consists of the heart, blood vessels, and blood. First described in 1628 by the english physician William Harvey, the main tasks of the CVS are to supply the cells and tissue with nutrients, oxygen, carbon dioxide (CO_2) and other essential elements as well as to dispose waste materials. Figure 2.1 shows a simplified diagram of the human circulatory system with its main arteries and veins.

The sources of the following section are Kaniusas [15], Lippert [17], Silbernagl and Klinke [35], and Thews et al. [41], if not stated otherwise.

2.1.1 The Heart

The heart is a muscular organ consisting of four cavities. The left heart with the left atrium and the left ventricle, and the right heart with the right atrium and the right ventricle. The left and the right heart are two pumps, divided by the cardiac septum, which are responsible for the blood flow through the human body. The right heart pumps the blood into the lung and the left heart through the rest of the body. The CVS is an enclosed system, therefore, the amount of blood per unit of time in the left and the right heart are equal.

The pumping of the heart is a rhythmic sequence which can be categorized into two phases, termed systole and diastole. The systole is the contraction of the two ventricles. In this phase, the ventricles contract and push the blood through the body, and the left and right atrium slacken and are filled with blood. In the diastole, the behaviour is contrary, hence, the atria are pumping the blood into the ventricles. The blood flow is pulsatile and not continuous, due to this rhythmic behaviour of the heart.

The walls of the four cavities do not have the same thickness due to different muscular mass. Both atria with a wall thickness of about $1.5\,\mathrm{mm}$ are thin compared to the two ventricles. The wall thickness of the right ventricle is $2\,\mathrm{mm}$ to $4\,\mathrm{mm}$ and of the left ventricle $8\,\mathrm{mm}$ to $11\,\mathrm{mm}$.
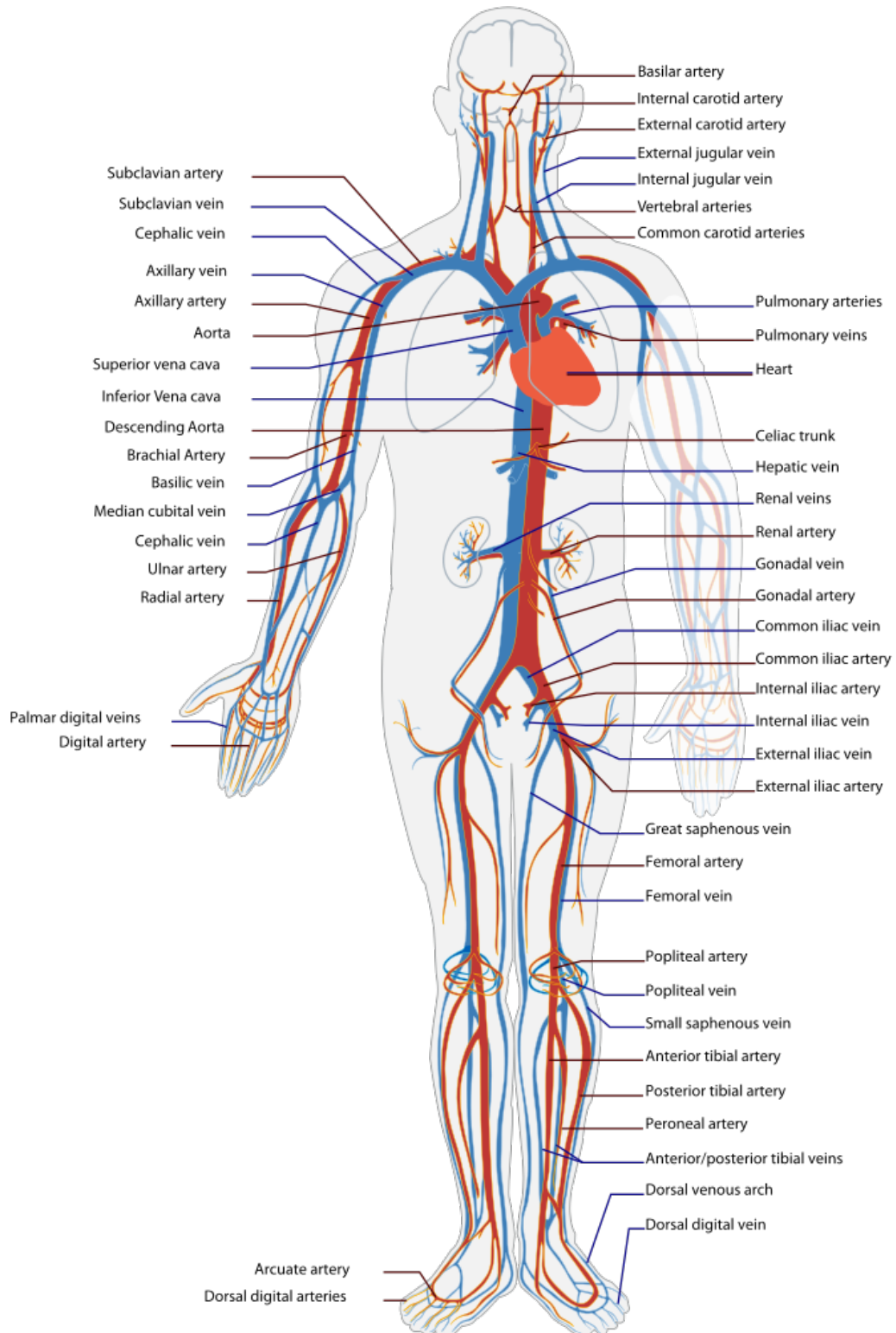
Figure 2.1: Simplified diagram of the human circulatory system in anterior view, showing the main arteries and veins (source: [43])

The difference can be explained by the different pressure produced by the ventricles. The left ventricle is part of the high-pressure system (see section 2.1.2.2) and therefore, must form a five times higher pressure than the right ventricle, which is on the contrary part, the low-pressure system, in order to overcome the pressure barrier to pump the blood through the arteries.

The size of the heart of an adult is about the size of a clenched fist. The weight of the heart for a grown-up man is approximately $320\,g$ and for a woman $280\,g$. The sequence of one systole and one diastole is one heartbeat. The heart rate *HR* is the number of heart beats per minute. In resting state the heart rate is about 70 beats per minute (bpm, $\min^{-1}$). The stroke volume (SV) is the amount of blood which is pumped through the heart during one contraction of the ventricles. It is about $70\,ml$. The cardiac output (CO) defines the amount of blood which is pumped through the body in one minute. It is the heart rate times the stroke volume and is approximately $5\,l$.

2.1.1.1 Blood flow through the heart

The blood flows through the heart in a certain direction which is assured by the four heart valves. Blood low on oxygen comes from the systemic circulation (see section 2.1.2.1) via the superior and inferior vena cava into the right atrium. Passing the tricuspid valve the blood flows into the right ventricle entering the pulmonary circulation (see section 2.1.2.1). Through the pulmonary valve the blood flows to the lung where it is oxygenated and from there into the left atrium. The mitral valve is passed. Then, the blood reaches the left ventricle, and from there it is pumped via the aortic valve and the aorta into the rest of the body, entering the systemic circulation. Figure 2.2 shows a schematic representation of the heart as well as the flow directions.

2.1.1.2 Coronary Circulation

The heart itself is supplied with blood like every other tissue in the body. The coronary circulation describes the supply of the heart muscle with oxygen and nutrients by the coronary vessels. Two main arteries branch off from the aorta, the left and right coronary artery, to supply the heart muscle. The left coronary artery supplies the left heart, a small part of the right heart and most of the cardiac septum. It is responsible for $80\,\%$ of the nourishment of the heart. The right coronary artery supplies most parts of the right heart. The exact coverage area of the coronary arteries underlies a considerable variability. The venous blood of the heart flows back to the right atrium mainly via the coronary sinus.

2.1.2 Circulatory Loops

2.1.2.1 Systemic and pulmonary circulation

The CVS can be categorized into the systemic and the pulmonary circulation. The left and the right heart have to pump the same blood volume per unit of time, but they have to pump the blood through different distances. The right heart pushes the blood through the lung to the left heart (pulmonary circulation), which is a shorter way than the one of the left heart pumping the blood through the rest of the whole body (systemic circulation). These two circulatory systems are consecutively parts of one circulatory system and thus, are not independent from each other.
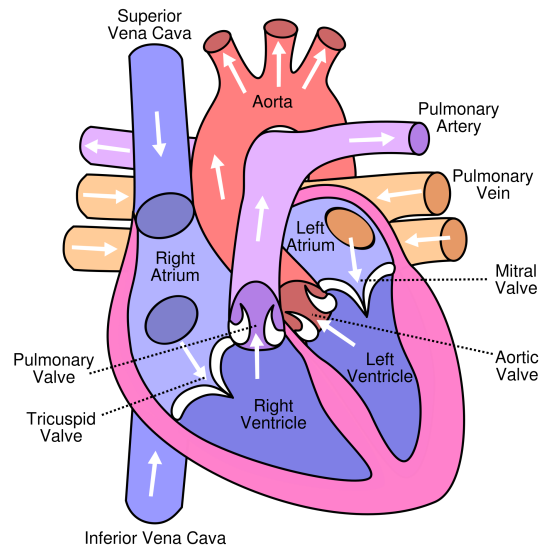
Figure 2.2: Diagram of the human heart showing the four cavities, the four valves, flow directions, and the inflowing and out-flowing vessels. (source: [45])

The systemic circulation starts at the left atrium and the left ventricle of the heart. Through the aorta the blood is transported to all organs and tissues where the exchange between blood and tissues takes place. Metabolic waste products diffuse into the blood and are carried to the liver and kidneys, and oxygen and nutrients diffuse from the blood into the tissues. Afterwards the blood flows back to the heart. The systemic circulation includes the coronary circulation (see section 2.1.1.2).

The pulmonary circulation starts at the right atrium and right ventricle where the de-oxygenated and CO_2-rich blood is pumped through the lung to the left heart. Due to the gas exchange in the lung the oxygen deprived blood is oxygenated as well as the CO_2 is released from the blood into the lung and leaves the body through respiration.

2.1.2.2 High-pressure and low-pressure system

The distance of the blood through the pulmonary circulation is much shorter than through the systemic circulation. Thus, lower pressure is sufficient to pump the blood from the right to the left heart through the lung. The pressure in the pulmonary artery is about $1/7$ of that in the aorta (mean pressure: $15\,\mathrm{mmHg}$ vs. $100\,\mathrm{mmHg}$).

The low-pressure system is not equal to the pulmonary system. Since the arterioles have the highest flow resistance, it begins with the capillaries. The low-pressure system compromises the capillaries, venules, veins, right atrium, right ventricle, the pulmonary vessels, the left atrium, and the left ventricle in diastole. The high-pressure system consists of the left ventricle in systole, arteries, and arterioles.
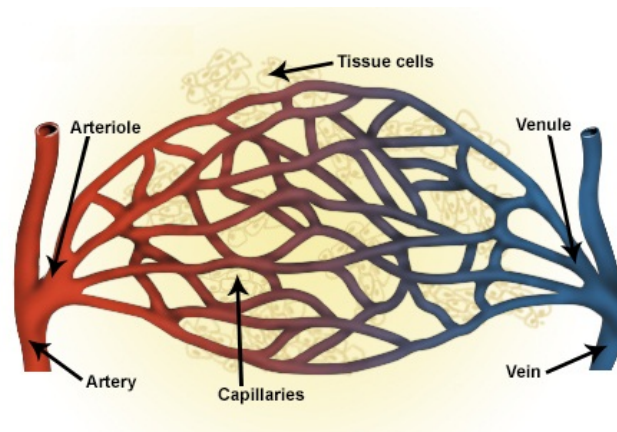
Figure 2.3: Illustration of blood vessels including artery, arteriole, capillaries, vein, and venule (source: [23])

2.1.3 Blood Vessels

The blood vessels are the transport system of the blood. In collaboration with the heart, the vessels transport the blood through the whole human body. They can be classified into arteries, arterioles, capillaries, venules, and veins (see figure 2.3). Figure 2.1 shows the CVS with its main arteries and veins.

The aorta, originating from the left ventricle of the heart, is the artery with the largest lumen of $25\,\text{mm}$. It branches into smaller arteries with a lumen of about $2\,\text{mm}$ and further into arterioles with a lumen of $20\,\mu\text{m}$. The capillaries are the blood vessels with the smallest inner diameter of $5\,\mu\text{m}$ to $20\,\mu\text{m}$. In comparison, an erythrocyte has a diameter of $7\,\mu\text{m}$. After the capillaries the vessels start to combine to venules ($30\,\mu\text{m}$) and moreover to veins ($2.5\,\text{mm}$) with the largest being the vena cava ($30\,\text{mm}$). With decreasing diameter the number of vessels is increasing.

The microcirculation compromises all parts where the exchange of substances takes place. These are the arterioles, capillaries, venules, lymphatic vessels, and the surrounding tissue. There the actual exchange of oxygen, CO_2, nutrients, and metabolic waste products between the blood and the tissue takes place.

Arteries transport blood away from the heart and veins towards the heart. Consequently, the definition of arteries and veins is based on the flow direction of the blood. It is common practice that the adjective *arterial* refers to oxygenated blood and the adjective *venous* refers to deoxygenated blood. Hence, it is often mistaken that all arteries transport oxygenated blood and all veins blood low in oxygen. The two exceptions are the pulmonary circulation and the placental circulation. Figure 2.4 is a schematic representation of the human circulatory system showing the circumstance of the pulmonary artery carrying blood low in oxygen and the pulmonary vein transporting oxygenated blood.

The pressure inside the vessels determines the wall thickness. The mean pressure (see section 2.2.1) in the vessels is highest in the aorta and becomes slightly lower as the distance to the left heart increases. The pulsatile part of the pressure increases first due to wave reflections,
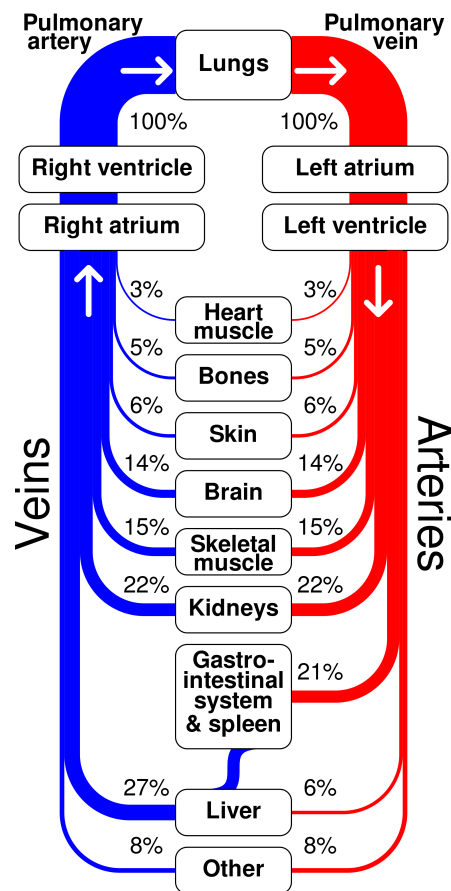
Figure 2.4: Diagram of the human circulatory system with approximate relative percentages of cardiac output delivered to major organ systems. Red is oxygenated blood, blue is oxygen depleted blood (source: [6])

but decreases and finally disappears after the blood passes the capillaries. Figure 2.5 shows the pressure distribution along the systemic circulation. Arteries and arterioles are part of the high-pressure system (see section 2.1.2.2) and therefore, have thicker walls than the vessels of the low-pressure system.

The wall of blood vessels is built by three main components which are elastin, smooth muscle, and collagen fibres. When the left ventricle contracts, high pressure is generated. Therefore, the arteries near to the heart are more elastic in order to withstand the high pressure and to smooth the blood flow. The closer a vessel is to the heart, the higher is the relative amount of elastin fibres of the wall. Figure 2.6 shows a pulse wave starting at the aortic valve at the left ventricle and propagating through a vessel.
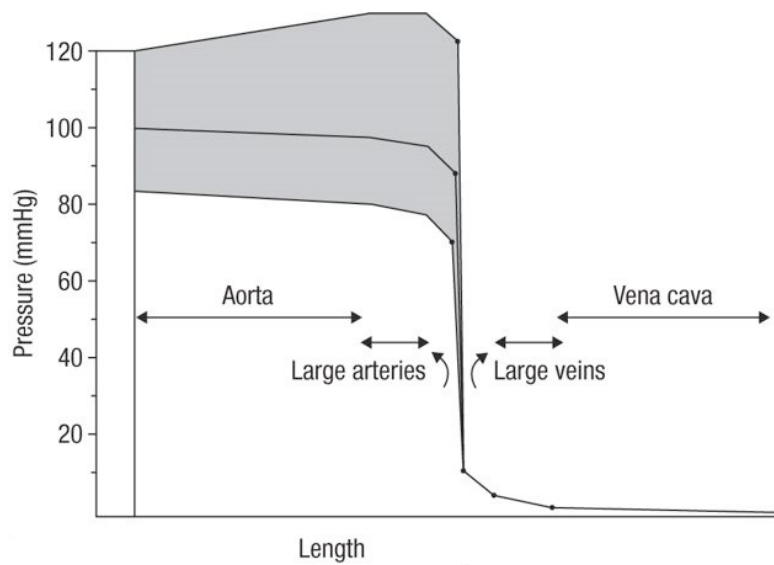
Figure 2.5: Pressure distribution along the systemic circulation. Mean pressure slightly decreases whereas the pulsatile part (grey area), the pulse pressure, increases due to wave reflections resulting in pulse pressure amplification (source: [24])
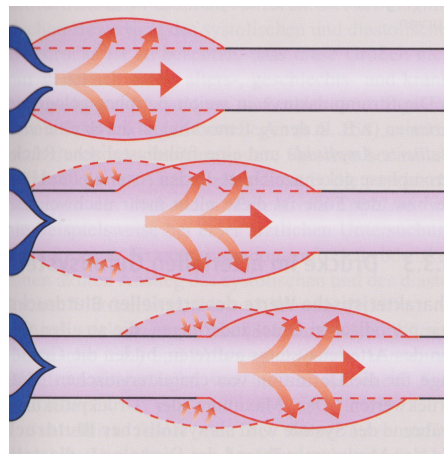

Figure 2.6: A pulse wave propagating from the left ventricle (source: [41])

2.1.4 Blood

Blood is a fluid and occurs in all organs. Due to its tasks it can be described as liquid body tissue. An adult has a blood volume of about 4 l to 6 l.

Blood consists of cells and plasma. There are three types of blood cells: Erythrocytes (red blood cells), leukocytes (white blood cells), and thrombocytes (blood platelets). The erythrocytes account for 99 % of the blood cells. The blood plasma consists of 90 % water and 10 % dissolved substances. The dissolved substances are electrolytes, proteins, and other organic

substances.

The haematocrit value describes the volume fraction of the blood cells compared to the whole blood volume. It is about 0.46 for men and 0.42 for women. The blood cells are mainly erythrocytes, hence, nearly half of the blood volume are red blood cells.

Blood is the universal means of transportation of the CVS and is responsible for the exchange of the following:

- *Blood gases*: The exchange from oxygen and CO_2 takes place in the whole body. Organs absorb oxygen and dispense CO_2, in the lung the behaviour is reverse.

- *Nutrients*: Blood absorbs carbohydrates, amino acids, fat, vitamins, and mineral substances and carries them from the source (e.g. intestine) to the target (organs).

- *Heat*: All chemical processes in the body produce heat. The blood stores the heat and transports it to the body surface where the heat is released to the surrounding.

- *Hormones*: The endocrine glands release the hormones into the blood. The blood carries them to all cells in the body. The cells for whom the messengers are intended for can absorb them.

- *Antibodies*: The blood carries antibodies, which are produced by the lymphatic system and white blood cells. They are responsible to fight intruders into the body like bacteria or a virus.

- *Water*: The blood is responsible for the water supply for all cells.

- *Slag materials*: The processes in the body produce a lot of waste materials. The blood transports them to the emunctories like the liver, lung, or kidneys.

2.2   Hemodynamic Parameters

Hemodynamics describes the fluid dynamics of blood flow in the CVS. It is a mainstream topic today and its roots go back to Harvey (1642-1727), Galileo (1564-1642) and Newton (1642-1727) [24]. There are many parameters describing the health status of the CVS and thus, can be useful for diagnosing cardiovascular diseases (CVDs). In the following section, the hemodynamic parameters which are discussed in the later sections in this work, are described. The sources for this section are Nichols et al. [24], Kaniusas [15], and Thews et al. [41], if not stated otherwise.

2.2.1   Blood Pressure

The blood inside a vessel exerts pressure on the wall of the vessel. This pressure is the blood pressure. The pressure levels, which are commonly spoken about, are from the arteries (high-pressure system). Since the heart pumps the blood in a certain rhythm, blood pressure is not constant, but a dynamic value. The *HR* is the speed of this rhythm, measured in beats per minute (min^{-1}). The highest pressure occurs when the left ventricle contracts. This peak in the pressure

curve is the systolic blood pressure *SBP*. The diastolic blood pressure *DBP* is the minimum value of the pressure wave. The difference of the systolic and diastolic value is the pulse pressure *PP* as defined in equation 2.1.

$$PP = SBP - DBP \tag{2.1}$$

Blood pressure is usually given in millimetre of mercury (mmHg), less often in kilopascal (kPa). Defined by the American Heart Association[1] normal blood pressure levels are less than $120\,\text{mmHg}$ systolic and less than $80\,\text{mmHg}$ diastolic when measured peripheral at the upper arm.

Apart from the maximum and minimum of the blood pressure curve, the mean value can be calculated as further characteristic parameter. This mean arterial pressure *MAP* is defined as integration of the blood pressure curve as seen in equation 2.2.

$$MAP = \frac{1}{t_c} \int_0^{t_c} P \, \mathrm{d}x \tag{2.2}$$

The duration of one cardiac cycle (one heartbeat) is t_c. The *MAP* can also be approximated whereas one possibility is shown in equation 2.3.

$$MAP \approx DBP + \frac{1}{3} PP. \tag{2.3}$$

There are two principle ways to measure arterial blood pressure (BP), which are direct and indirect. The direct method is invasive. After puncturing an artery, the measuring instrument is inserted into the vessel with a cannula or catheter. This allows a continuous recording of the pressure curve and exact determination of the different BP levels. Since the invasive method is expensive as well as not pleasant for the patient, the indirect (noninvasive) method is normally used in clinical routine. The indirect method uses a blood pressure cuff which is usually placed at the upper arm or wrist.

BP levels which are measured at the arm are referred to as *peripheral* values. Hence, the different parameters get the term *peripheral* preceded. There are peripheral systolic blood pressure *pSBP*, peripheral diastolic blood pressure *pDBP*, peripheral pulse pressure *pPP*, and peripheral mean arterial pressure *pMAP*. BP levels at the aorta are termed as *central* values. Thus, there are central systolic blood pressure *cSBP*, central diastolic blood pressure *cDBP*, and central pulse pressure *cPP*. They are also often labelled as *aortic* values.

The pressure wave form at the aorta is not the same as in the peripheral sites. It changes when the wave travels along the arteries from the left ventricle on. These alterations are mainly due to wave reflections. Figure 2.7 shows the change of the pressure curve. One noticeable aspect is the elevated pulse pressure in the periphery (which can be also seen in figure 2.5). The pulse pressure amplification *PPamp* describes this behaviour and is defined as the ratio of *pPP* to *cPP* as defined in equation 2.4.

$$PPamp = \frac{pPP}{cPP} \tag{2.4}$$
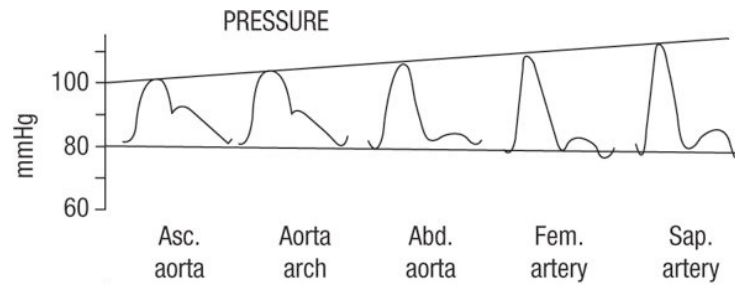
---

[1] http://www.heart.org/HEARTORG/

Figure 2.7: The pressure wave changes its form when traveling along the arteries. The systolic blood pressure level increases, hence, the pulse pressure is elevated in the periphery (source: [24])
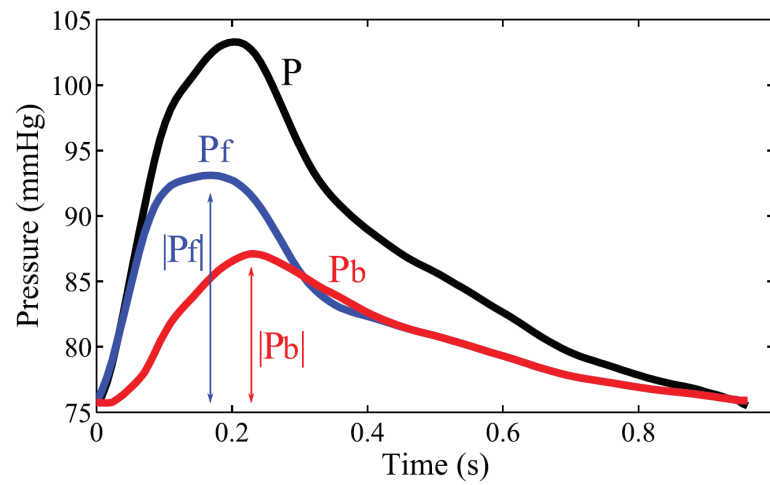

Figure 2.8: Measured pressure wave P is the sum of the forward pressure wave and the backward pressure wave (source: [30])

2.2.2 Reflection Magnitude

The pulse wave generated by the heart, representing the forward component, travels along the vascular pathway. At peripheral sites the pressure wave is reflected and a backward pressure wave returns towards the heart. Reflection is caused by branching and narrowing of the vessels. The measured pulse wave is the sum of the forward pressure wave P_f and the backward pressure wave P_b [52], as shown in figure 2.8. The reflection magnitude RM is a parameter describing the extent of the reflection. It is defined as the amplitude ratio of the backward pressure wave and the forward pressure wave [10] as defined in equation 2.5.

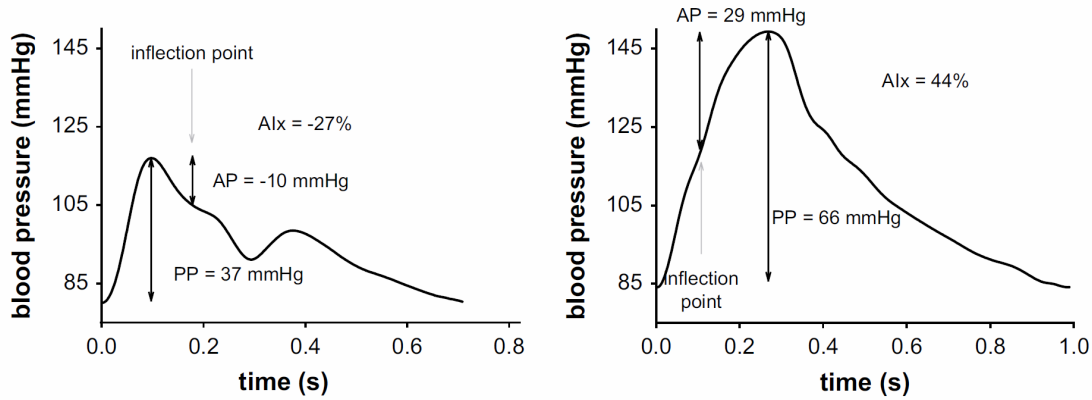$$RM = \frac{\max(P_b) - \min(P_b)}{\max(P_f) - \min(P_f)} = \frac{|P_b|}{|P_f|} \qquad (2.5)$$

Figure 2.9: Left: Reflected wave returns in late systole leading to a negative augmentation pressure and negative augmentation index. Right: Systolic peak pressure is augmented due to the reflected wave returning earlier which results in a positive augmentation pressure and augmentation index (source: [38])

2.2.3 Augmentation Index

The augmentation index *AIx* is a parameter describing the effect of the returning wave from the periphery. In contrast to the reflection magnitude, the augmentation index is not solely dependent on the amplitude, but also on the timing of the reflected pressure wave. The inflection point marks the position where the reflected wave starts to effect the forward wave. In figure 2.9 there are two different pressure wave forms displayed. In the left curve, the inflection point is after the systolic peak, whereas in the right curve the reflected wave returns earlier and the inflection point is before the systolic peak.

The augmentation pressure *AP* is defined as the difference of the systolic peak and the pressure level at the inflection point. If the reflected wave returns late in the systole, the inflection point is after the systolic peak. In this case, the augmentation pressure is defined to be negative, like shown in the left pressure curve of figure 2.9. Whereas, if the inflection point is before the systolic peak, the augmentation pressure is positive. The augmentation index, as shown in equation 2.6, is defined as the ratio of the augmentation pressure and the pulse pressure and commonly given in percent.

$$AIx = \frac{AP}{PP} * 100 \tag{2.6}$$

The *AIx* depends on different factors with one being the *HR* [54]. Thus, the *AIx* is often normalized to a *HR* of $75 \, \text{min}^{-1}$ termed as augmentation index at $75 \, \text{min}^{-1}$ *AIx@75*. Other influencing factors are the arterial stiffness, age, height, gender, cardiac output, stroke volume, left ventricular ejection time, and the quality of the identification of the inflection point.

The *AIx* can be determined at different sites, depending on where the pressure wave is recorded. There are for example carotid, aortic (central), or peripheral *AIx*. In this work, always the aortic *AIx* is meant, if not stated otherwise.

2.2.4 Pulse Wave Velocity

The speed of the pressure wave generated by the heart is termed as pulse wave velocity *PWV*. The pressure wave is spreading via momentum transfer from particle to particle. Hence, the speed of the pressure wave is much higher than the speed of the blood stream. Typical values range from $5\,\mathrm{m\,s}^{-1}$ to $15\,\mathrm{m\,s}^{-1}$. Figure 2.6 shows a pulse wave generated from the ventricle and spreading through the artery. *PWV* is the gold standard to determine arterial stiffness [24, 2, 4].

There are a lot of different possibilities to determine the *PWV*. They can be divided into invasive and noninvasive methods, whereas noninvasive methods are better getting along with the daily clinical routine and therefore are preferred instead of invasive ones. An invasive method is cardiac catheterization. With the catheter, the pulse wave is invasively recorded at two different sites, for example at the ascending aorta and at the aortic bifurcation. The distance is divided by the travel time between these two recording sites.

The principle of the noninvasive method is the same as for the invasive measurement. The pressure wave is recorded at two different sites, for example at the carotid artery and the femoral artery, with for instance a tonometric or an oscillometric approach. The distance is divided by the travel time between these two sites. This leads to the carotid-femoral *PWV* (cf-*PWV*). A further possibility is the brachial-ankle *PWV*. The determining of the distance between the two measurement sites is an issue of the noninvasive methods because it is difficult to determine the exact distance along the arterial tree [48, 49]. Nevertheless, noninvasive methods are delivering trustworthy results [9].

The *PWV* depends of the character of the vessel (composition of the wall, wall thickness, diameter). Clinically most interesting is the determination of the stiffness of the aorta, hence, the *PWV* of the aorta is of great interest. Additionally, it would be more pleasant for the patients, if the recording of the pulse wave on one site is sufficient instead of recording at two sites. The Mobil-O-Graph (see section 3.2) records the pressure wave on the upper arm and uses a generalized transfer function to compute the aortic pressure wave. Wave separation is applied on the aortic pressure wave and the age, central pressure, and aortic characteristic impedance are used in order to obtain the aortic *PWV* [8]. Hence, in this work the aortic *PWV* is discussed, if not declared otherwise.

Data Acquisition

3.1 Study Design

In Luebeck, Germany, a healthy population cohort was recruited where all subjects stated no drug intake, no dyslipidemia, no mental disorders, no electrocardiography (ECG) abnormalities, no diabetes, and no hypertension. The Institutional Ethics Committee gave approval and all participants gave informed consent. The study was in agreement with the Declaration of Helsinki.

3.2 Mobil-O-Graph

The device used in this study is the Mobil-O-Graph from I.E.M. GmbH, Stolberg, Germany. It is a 24 hour oscillometric pulse wave analysis (PWA) monitor. The Mobil-O-Graph is the first device which is combining pulse wave analysis (PWA) and ambulatory blood pressure monitoring (ABPM). Additionally, to the common 24-hour assessment of peripheral blood pressure, central hemodynamic parameters can be evaluated over 24 hours as well. There are several devices which enable 24-hour peripheral blood pressure monitoring or other devices, which allow the noninvasive recording of central hemodynamic parameters [21].

In order to obtain the central hemodynamic parameters the Mobil-O-Graph uses the ARC-Solver method [47], developed by the AIT Austrian Institute of Technology, Vienna, Austria, to reconstruct the central pulse wave [46]. The measurements are made with a common cuff which the experimentees are wearing on the upper arm. A conventional blood pressure measurement is executed at the arteria brachialis. Afterwards, the cuff is again inflated at the peripheral diastolic blood pressure for about $10\,\mathrm{s}$ where the recording of the pulse wave takes place. A generalized transfer function is applied to obtain the central pulse wave and furter, central hemodynamic parameters. The device has been successfully validated [51, 50].

The Mobil-O-Graph was programmed to make measurements every 15 minutes from 8 A.M. till 11 P.M. and every 30 minutes from 11 P.M. to 8 A.M. If the recording of the BP or the

pulse wave is not successful there are no measured values for this point in time, the data fields which are stored by the Mobil-O-Graph stay empty. The Mobil-O-Graph analyses and rates the recorded peripheral pulse wave. A measurement quality from 1 to 3 classifies the quality of the recording with measurement quality one being the best.

The data record from the Mobil-O-Graph is exported as Excel file[1] (.xls), hence, there is one Excel file per participant. The Excel files from all experimentees are combined and transferred into one MATLAB structure array. For unsuccessful measurements Not a Number (NaN) is stored in the structure array. All data processing, plotting, and statistical analysis have been done with MATLAB[2] (R2015b).

---

[1] Microsoft Excel, www.microsoft.com
[2] The MathWorks, Inc., www.mathworks.com

Methods

4.1 Data Preprocessing

The data preprocessing compromises the removal of experimentees, the removal of unsuccessful PWA measurements, and the restriction to 24 hours. First the measurements from all participants have been analysed if all data records fit the demands for the data evaluation (see section 4.1.1). Thereafter, the preprocessing steps as illustrated in figure 4.1 are executed before every further data evaluation and plotting.
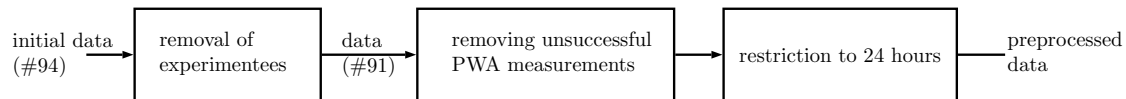

Figure 4.1: Data preprocessing

4.1.1 Removal of experimentees

The data record of every experimentee has been analysed to evaluate if the measurements are proper to be used in 24-hours evaluations. All experimentees must have measurements distributed over 24 hours, especially there must be measurements during daytime and nighttime for the day/night evaluation. First all unsuccessful measurements are removed (see section 4.1.2). Thereafter, for every experimentee the following information is determined:

■ the measurement quality average and its standard deviation of the data record

■ the different hours where at least one measured value exists

■ the number of measurements

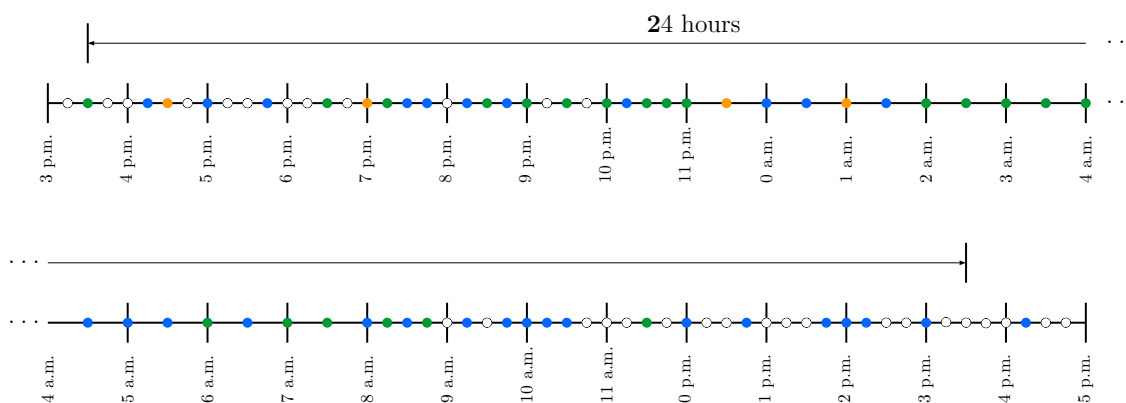■ the overall duration of the data record

Figure 4.2: Representative Mobil-O-Graph measurements of one experimentee. Green: measurement quality 1, Blue: quality 2, Orange: quality 3, Empty: no successful PWA

The initial data contains 94 experimentees. Two records are from the same subject with half a year in between. The latter record is removed because its average measurement quality is worse, there are measurements in less different hours (18 vs 21), and the single measurements are not as evenly distributed over 24 hours as in the earlier one. The biggest gap of the first record is from 9:30 A.M. to 11:45 A.M., whereas from the second record it is from 10:30 A.M. to 4:00 P.M.

Further two participants are taken out because both have measurements for less than 12 different hours. Additionally one has no data from 10:00 P.M. to 10:00 A.M., hence, no day/night assessment can be done. Thus, the final data record consists of 91 subjects.

The data has been also analysed considering only measurement quality 1 and 2. This leads to no different results as with considering measurement quality 3 too.

4.1.2   Removing unsuccessful PWA measurements

The Mobil-O-Graph executes PWA measurements in certain intervals (see section 3.2). If the measurement was not successful, no values are available. Instead Not a Number (NaN) is stored in the record in the MATLAB structure array. Figure 4.2 shows a representative data record of one experimentee, illustrating the different measurement intervals between day and night, and the different measurement qualities. In a first preprocessing step, all unsuccessful measurements are removed from the MATLAB structure array.

4.1.3   Restriction to 24 hours

The experimentees got instruction to do PWA recordings for at least 24 hours. About one third of the data records of the participants are slightly longer than 24 hours. Thus, all data records are restricted to exactly 24 hours. The first measurement is identified and from this point in time on after 24 hours all further measurements are deleted, which is illustrated in figure 4.2.

About two third of the data records are equal or less than 24 hours. These recordings remain unchanged.
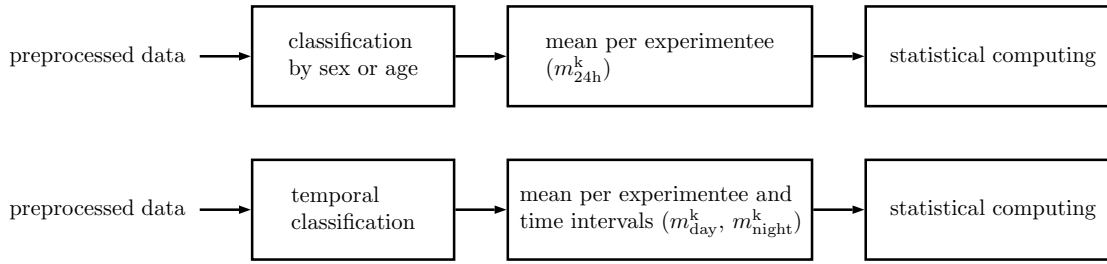
Figure 4.3: Schematic representation of the data evaluation when dividing the cohort by sex or age, or temporal

4.2 Data Evaluation

Functions have been implemented to classify the cohort by sex, age, and temporal. Any time interval within 24 hours can be extracted, which is used to get a day and night interval. Likewise, the cohort can be divided into any desired age intervals. The data has not been smoothed for the evaluation as it is done for the 24-hour plots (see section 4.3.1.1). Figure 4.3 shows the schematic representation of the data evaluation.

Further functions have been developed to compute the corresponding mean values and to execute the statistical analysis. For all computations the measurement quality has been restricted to 2, hence, measurement quality 1 and 2 have been taken into account, quality 3 has been discarded.

4.2.1 Men vs Women

The data has been classified into men and women. For every experimentee and each parameter the mean over 24 hours m_{24h}^k as shown in equation 4.1 has been calculated.

$$m_{24h}^k = \frac{1}{n^k} \sum_{l=1}^{n^k} m^{k,l} \tag{4.1}$$

with

$\quad m_{24h}^k$ ...24 hour mean value per experimentee

$\quad m^{k,l}$ ...single measurement per experimentee

$\quad n^k$ ...number of single measurements per experimentee

$\quad k = 1, 2, \ldots, 91 \quad$ number of experimentees

$\quad l = 1, 2, \ldots, n^k \quad$ running index over the single measurements per experimentee

In order to compare the 24h mean values of the two groups, statistical analyses have been executed for every parameter. The results are shown in section 5.2.

4.2.2 Daytime vs Nighttime

The data has been examined for day and night differences. Dividing the data further into smaller intervals is not recommended because this leads to limited reproducibility [20]. In order to be able to assess differences between day and night, corresponding intervals have been defined. The aim was to get rid of the transition phases, which are the intervals, where the experimentees wake up or fall asleep. These phases differ from experimentee to experimentee. Therefore, the intervals have been defined at times where it is assumed that every study participant has been awake or asleep. The day interval begins at 9:00 A.M. and ends at 9:00 P.M., the night interval is from 0:00 A.M. to 6:00 A.M. [19]

The data has been divided into daytime and nighttime intervals. For every experimentee and each parameter the means of the daytime $m_{\mathrm{day}}^{\mathrm{k}}$ and the nighttime $m_{\mathrm{night}}^{\mathrm{k}}$ as shown in equation 4.2 and 4.3, respectively, have been calculated.

$$m_{\mathrm{day}}^{\mathrm{k}} = \frac{1}{n_{\mathrm{day}}^{\mathrm{k}}} \sum_{l=1}^{n_{\mathrm{day}}^{\mathrm{k}}} m^{\mathrm{k,l}} \tag{4.2}$$

with

$m_{\mathrm{day}}^{\mathrm{k}}$ . . .mean value of the day interval per experimentee

$n_{\mathrm{day}}^{\mathrm{k}}$ . . .number of measurements during the day interval per experimentee

$l = 1, 2, \ldots, n_{\mathrm{day}}^{\mathrm{k}}$ running index over the single measurements of the day

$$m_{\mathrm{night}}^{\mathrm{k}} = \frac{1}{n_{\mathrm{night}}^{\mathrm{k}}} \sum_{l=1}^{n_{\mathrm{night}}^{\mathrm{k}}} m^{\mathrm{k,l}} \tag{4.3}$$

with

$m_{\mathrm{night}}^{\mathrm{k}}$ . . .mean value of the night interval per experimentee

$n_{\mathrm{night}}^{\mathrm{k}}$ . . .number of measurements during the night interval per experimentee

$l = 1, 2, \ldots, n_{\mathrm{night}}^{\mathrm{k}}$ running index over the single measurements of the night

The day and night values have been compared with a paired statistical test. Further, the day and night interval have been analysed over the age of the experimentees. For this purpose, every day and night value has been combined with the age of the experimentee, resulting in two tuples per subject as shown in equation 4.4 and 4.5.

$$(age^{\mathrm{k}}, m_{\mathrm{day}}^{\mathrm{k}}) \dots \text{day tupel} \tag{4.4}$$

$$(age^{\mathrm{k}}, m_{\mathrm{night}}^{\mathrm{k}}) \dots \text{night tupel} \tag{4.5}$$

with

$$m_{\mathrm{day}}^{\mathrm{k}} \dots \text{mean value of the day interval per experimentee}$$

$$m_{\mathrm{night}}^{\mathrm{k}} \dots \text{mean value of the night interval per experimentee}$$

$$age^{\mathrm{k}} \dots \text{age of experimentee}$$

For the day as well as for the night tupel Pearson's correlation coefficient (R) with the $95\,\%$ confidence interval (CI) has been calculated. The results are shown in section 5.3.

4.2.3 Age-related Evaluation

The distribution of age and sex of the cohort has been analysed (see figure 4.4). The aim has been to get age groups with evenly distributed number of experimentees. As a consequence, the following three age groups were defined in order to get a young, middle, and elderly group:

- 20 to 29 years, 40 experimentees (13 men, 27 women)

- 30 to 49 years, 28 experimentees (13 men, 15 women)

- 50 to 69 years, 23 experimentees (10 men, 13 women)

The data has been divided into the 3 age groups. Afterwards, for every experimentee and each parameter the mean over 24 hours $m_{\mathrm{24h}}^{\mathrm{k}}$ has been calculated like stated in equation 4.1. In order to statistically compare the 3 classes, an analysis of variance (ANOVA) has been executed. If the null hypothesis, all 3 age groups are equal, has been rejected, a post-hoc analysis has been performed. The results are shown in section 5.4.
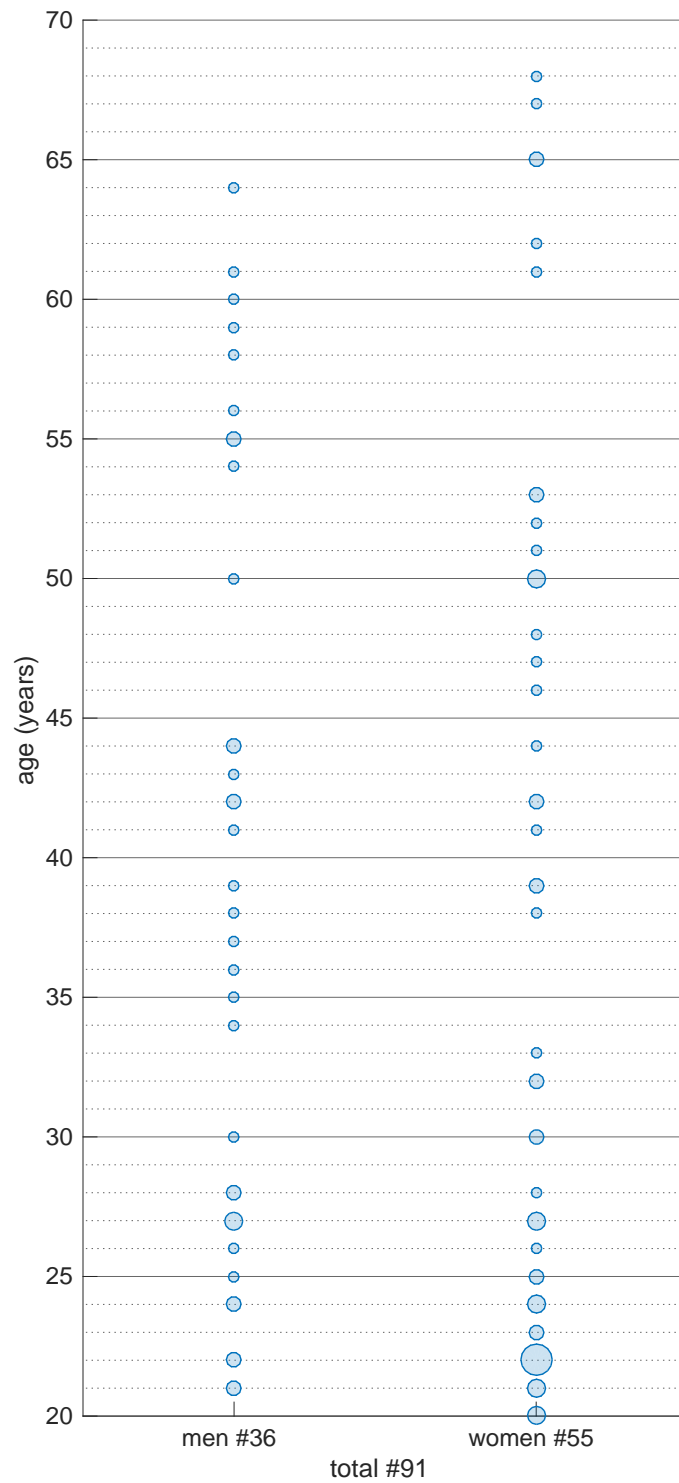
Figure 4.4: Distribution of age and sex of the population cohort. The size of the markers indicates the number of experimentees.

4.3 Graphical Representation

The graphical representation of the data happens in two different forms. One being 24-hour plots when classifying by age or sex, described in section 4.3.1, and the other being scatter plots for the day/night assessment described in section 4.3.2. The computations which are necessary for the graphical representation are restricting the measurement quality to 1 and 2, like it is done for the data evaluation (see section 4.2).

4.3.1 24 Hour Plots

The hemodynamic parameters have been visually analysed over 24 hours when classified by sex and by age. For the purpose of plotting graphs over 24 hours the data was smoothed over 3 hours (see section 4.3.1.1), otherwise the plotted curves would be considerably pronounced zigzag curves. Furthermore, a reference value has been computed in order to visualise the 24-hour mean value per class and to show the impact of the fact, that not every participant has measurements for every hour of the day (see section 4.3.1.2).

   Figure 4.5 shows the process of the 24-hour plotting. First, the data has been classified by sex or age. Next, the measurements of the classes have been smoothed, and the mean and reference values per hour have been calculated. The mean and reference values have been used to generate the 24-hour plots.
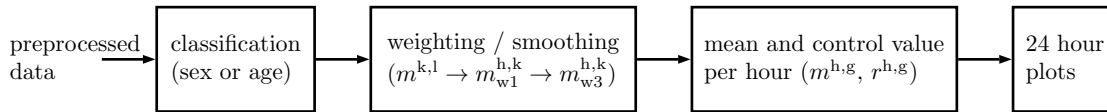
Figure 4.5: Schematic representation of the process for the 24-hour plotting

4.3.1.1 Weighting / Smoothing

The hemodynamic parameters are plotted over 24 hours. There are up to four measurements per hour per experimentee (see figure 4.2). Plotting every single measurement value of a parameter over 24 hours would result in a considerable zigzag curve, hence, before plotting, the data is smoothed.

   The smoothing process consists of two steps as illustrated in figure 4.6. First, for every hour and for each experimentee one data point is calculated by computing the mean of the single measurement values of the corresponding hour as stated in equation 4.6. The number of single measurements per hour and per experimentee $n^{h,k}$ ranges from 0 to 4. If an experimentee does not have a single measurement for an hour, NaN is stored for this hour.

$$m_{w1}^{h,k} = \begin{cases} \text{NaN} & \text{for } n^{h,k} = 0 \\ \frac{1}{n^{h,k}} \sum_{l=1}^{n^{h,k}} m^{k,l} & \text{for } n^{h,k} > 0 \end{cases} \tag{4.6}$$

   with

$m_{\mathrm{w1}}^{\mathrm{h,k}}$ ...mean value per hour and per experimentee weighted over 1 hour

$n^{\mathrm{h,k}}$ ...number of single measurements in hour h per experimentee

$\quad h = 1, 2, \ldots, 24$ hour of the day

$\quad l = 1, 2, \ldots, n^{\mathrm{h,k}}$ running index over the single measurements in hour h per experimentee

In a second step, the data is further smoothed. The value per hour h is computed by taking the mean value of the before hourly weighted values ($m_{\mathrm{w1}}^{\mathrm{h,k}}$) of the corresponding hour and the hour beforehand and afterwards, as stated in equation 4.7. This range from $h - 1$ to $h + 1$ goes seamless over midnight as shown in figure 4.6. The number of values which are taken into account for the second smoothing step per hour $n_{\mathrm{w1}}^{\mathrm{h,k}}$ ranges from 0 to 3. If $n_{\mathrm{w1}}^{\mathrm{h,k}} = 0$ than NaN is stored for the corresponding hour.

$$m_{\mathrm{w3}}^{\mathrm{h,k}} = \begin{cases} \mathrm{NaN} & \text{for } n_{\mathrm{w1}}^{\mathrm{h,k}} = 0 \\ \dfrac{1}{n_{\mathrm{w1}}^{\mathrm{h,k}}} \sum_{l=1}^{n_{\mathrm{w1}}^{\mathrm{h,k}}} m_{\mathrm{w1}}^{\mathrm{h,k}} & \text{for } n_{\mathrm{w1}}^{\mathrm{h,k}} > 0 \end{cases} \tag{4.7}$$

with

$m_{\mathrm{w3}}^{\mathrm{h,k}}$ ...mean value per hour and per experimentee weighted over 3 hours

$n_{\mathrm{w1}}^{\mathrm{h,k}}$ ...number of measurements, weighted over 1 hour, per hour h in the range of $h - 1$ to $h + 1$

$\quad l = 1, 2, \ldots, n_{\mathrm{w1}}^{\mathrm{h,k}}$ running index over the measurements weighted over 1 hour

After the smoothing process every experimentee has one measurement value per hour or in the exceptional case no value per hour. The final values which are plotted are obtained by taking the mean of the over 3 hours weighted values ($m_{\mathrm{w3}}^{\mathrm{h,k}}$) of the subjects of one group per hour as shown in equation 4.8.

$$m^{\mathrm{h,g}} = \frac{1}{n^{\mathrm{h,g}}} \sum_{k=1}^{n^{\mathrm{h,g}}} m_{\mathrm{w3}}^{\mathrm{h,k}} \tag{4.8}$$

with

$m^{\mathrm{h,g}}$ ...mean value per group and per hour

$n^{\mathrm{h,g}}$ ...number of experimentees having a value in hour h per group

$\quad n^{\mathrm{g}}$ ...number of groups

$\quad k = 1, 2, \ldots, n^{\mathrm{h,g}}$ running index over the experimentees having value in hour h per group

$\quad g = 1, 2, \ldots, n^{\mathrm{g}}$ running index over the groups
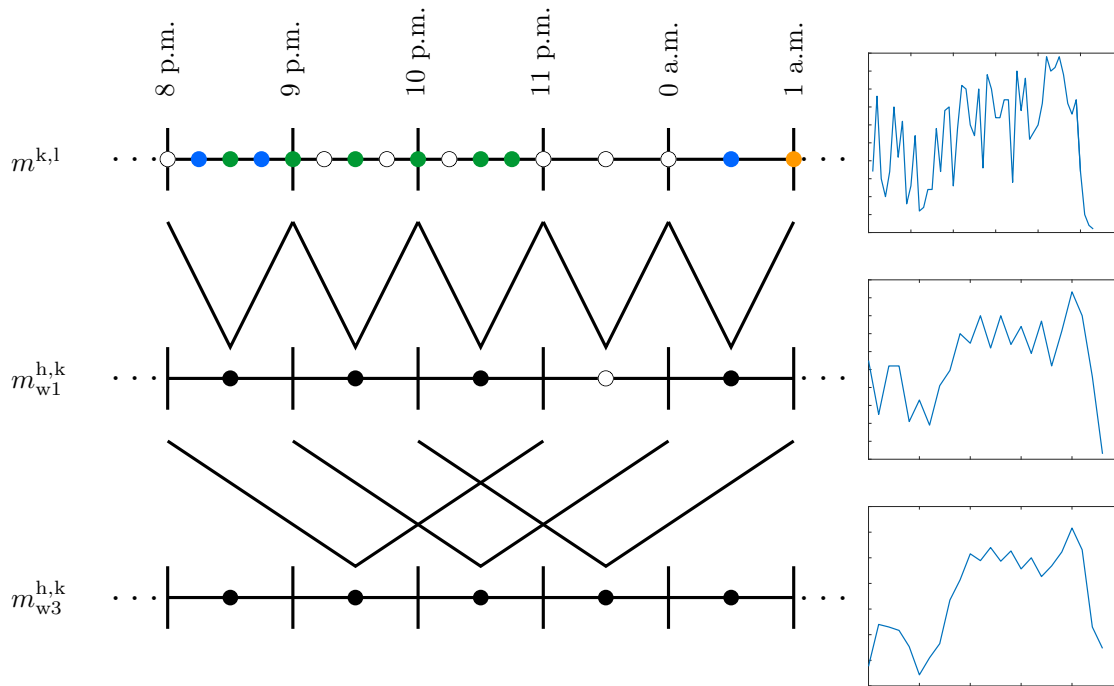
Figure 4.6: The smoothing process per experimentee is illustrated. First the measurements are smoothed over 1 hour by calculating the average value of the single measurements. In a second step the measurements are weighted over 3 hours by computing the mean value of the before hourly weighted values.

4.3.1.2 Reference Value

Not necessarily every experimentee has a value for every hour of the day after the weighting process, therefore, $n^{h,g}$ is not a constant value but dependent on the hour of the day. Thus, in different hours of the day not always the same experimentees are taken into account for the calculation of the mean value $m^{h,g}$. Figure 5.1 and 5.24 show the change of the number of experimentees over 24 hours when the data is filtered by sex or age, respectively. In order to see if and how the parameter is influenced by the change of experimentees from one hour to the next, a reference value has been calculated per group and per hour, and plotted along with the parameter. The reference value per hour and group $r^{h,g}$ is the average value of the 24-hours mean m^{k}_{24h} of the experimentees having a measurement value for this hour, as stated in equation 4.9.

$$r^{h,g} = \frac{1}{n^{h,g}} \sum_{k=1}^{n^{h,g}} m^{k}_{24h} \tag{4.9}$$

with

$r^{h,g}$ . . .reference value per group and per hour

m_{24h}^{k} . . .24 hour mean value per experimentee

$n^{h,g}$ . . .number of experimentees having a value in hour h per group

n^{g} . . .number of groups

$k = 1, 2, \ldots, n^{h,g}$ running index over the experimentees having value in hour h per group

$g = 1, 2, \ldots, n^{g}$ running index over the groups

Figure 4.7 illustrates the process of computing the data for plotting including the reference value for one class with three experimentees for the 24-hour plots.
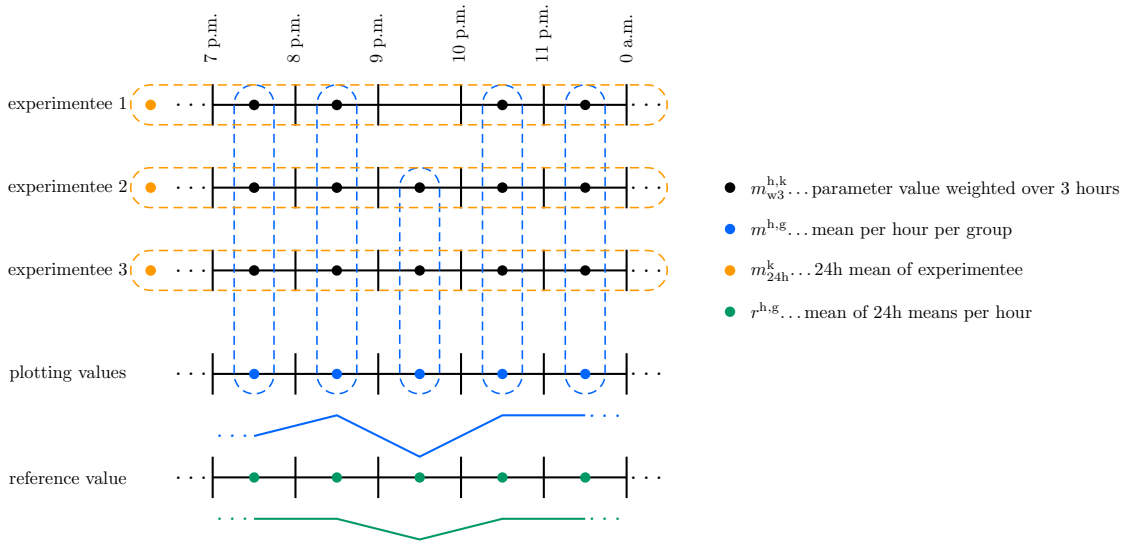
Figure 4.7: Example with 3 experimentees for calculating the data for one class with the corresponding reference value for the 24-hour plots. Per hour the mean value of all experimentees is computed. Furthermore, the mean of the 24-hour means per hour is calculated considering all experimentees who have a measurement value for this hour.

4.3.2   Day/Night Plots

The procedure to obtain the day/night plots is illustrated in figure 4.8. The specified day and night intervals have been extracted from the data. For every experimentee the mean of the daytime and nighttime interval have been calculated like it is done for the data evaluation in equation 4.2 and 4.3. Hence, every participant has a value for the day (m_{day}^{k}) and for the night (m_{night}^{k}).

The day/night plots are scatter plots. Every day and night value has been combined with the age of the participant in order to display the parameter values over age like it is done for the data

```
preprocessed ──→ classification ──→ mean per ──→ forming tuple ──→ scatter
data             (day and night)     day and night   (age^k, m_day^k)    plots
                                      (m_day^k, m_night^k)   (age^k, m_night^k)
```
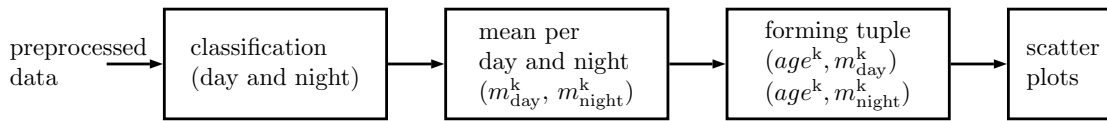
Figure 4.8: Schematic representation of the process of day/night plotting

evaluation in section 4.2.2. Hence, the two tuple like stated in equation 4.4 and 4.5 are plotted for every experimentee. Additionally, a linear regression line for the day and night values has been computed and drawn into the plot in order to see the trend of the parameters over age more clearly.

4.4 Statistical Analysis

The statistical analysis has been done with MATLAB (R2015b). Normally distributed data is displayed as mean $\pm$ SD and non-normally distributed data as median and interquartile range (IQR).

In order to compare two samples the parametric two-sample t-test has been used. For comparing men with women the unpaired t-test has been used and for the day/night assessment the paired t-test has been applied. The assumptions of the unpaired test are that the samples are normal distributed and have equal variances. The same accounts for the paired test except that the assumptions must apply to the difference of the two data samples. The Kolmogorov-Smirnov test has been used to test for normal distribution and the F-test has been used to test for equal variances. If the variances are not equal but the samples are normal distributed, the Welch's t-test has been used. If the data is not normal distributed a log transformation is applied. Is the data normal distributed after the log transformation the corresponding test has been executed with the log transformed data. If the data is again not normal distributed, neither without transformation nor log-transformed, the nonparametric Mann-Whitney U test (also called Wilcoxon rank-sum test) has been applied.

Since there are three groups which must be compared when classifying the data by age, the analysis of variance (ANOVA) has been used. The assumptions of the ANOVA are normal distribution of the samples and that the groups have equal variances. In order to test for equal variances, the Levene's test has been applied. If the variances differ between the groups, the Welch's ANOVA has been used. If the result of the ANOVA states that the groups are not equal than a post-hoc analysis is performed to find out, which group differ from each other. After the ANOVA the Tukey-Kramer method has been used and after the Welch's ANOVA the Games-Howell test has been applied.

An α level of $5\,\%$ ($p \leq 0.05$) is assumed to be significant and has been used for all statistical tests. In the chapters results (5) and discussion (6), $p < 0.001$ is stated as highly significant.

CHAPTER 5

Results

5.1 Demographic characteristics of the study participants

Table 5.1 lists the main characteristics of the whole population as well as separated for men and women. The 91 experimentees consist of 36 men and 55 women. The average age is $36.8\,\mathrm{years}$ with a total range from $20\,\mathrm{years}$ to $68\,\mathrm{years}$, the median age is $33\,\mathrm{years}$. All data is normal distributed except the age, which is normal distributed after a log-transformation. Hence, the weight, height, BMI, and age have been compared with the two-sample t-test (unpaired). Men are highly significant ($\mathrm{p} < 0.001$) taller and heavier than women. Although not significant men have a higher mean of the body mass index (BMI)[1] and a higher median of the age than women.

Table 5.1: The demographic data of the population cohort by sex. The values are the mean $\pm$ SD except for the number of experimentees, where the number and corresponding percentage is given, and for the age the median and the interquartile range is given.

	All	**Men**	**Women**	**p**
# exp (%)	91 (100)	36 (39.6)	55 (60.4)	
age (years)	$33\,(24-49.5)$	$37.5\,(27-52)$	$30\,(22-47.75)$	0.182
weight (kg)	72.71 ± 12.62	80.78 ± 10.85	67.43 ± 10.83	<0.001
height (m)	1.74 ± 0.09	1.81 ± 0.06	1.69 ± 0.06	<0.001
BMI ($\mathrm{kg\,m}^{-2}$)	24.11 ± 3.82	24.65 ± 3.54	23.76 ± 3.99	0.278

5.2 Men vs Women

The *HR* of men ($67.56 \pm 8.57\,\mathrm{min}^{-1}$) was significantly lower ($\mathrm{p} = 0.01$) than of women ($71.88 \pm 7.05\,\mathrm{min}^{-1}$). Figure 5.2 shows the diurnal profile of the *HR*, having its minimum for both men

---

[1] $BMI = \frac{mass(kg)}{height^2(m)}$

and women between 4 A.M. and 5 A.M., then it steeply ascends until 10 A.M. After that, men reaching a plateau whereas the *HR* of women increases further until 5 P.M. From there on the *HR* of men and women descends until 4 A.M. All blood pressure levels (*pSBP*, *pDBP*, *pMAP*, *cSBP*, and *cDBP*) were significantly higher in men than in women except the peripheral and central pulse pressure, where no significant difference ($p \leq 0.05$) was found. Figure 5.3, 5.4, 5.5, and 5.7 show the behaviour over 24 hours of the *pSBP*, *pDBP*, *pMAP*, and *cSBP*, respectively, showing for all pressures a minimum plateau from 2 A.M. to 5 A.M. Thereafter, all pressure levels increase until midday and reach a plateau until about 8 P.M. Afterwards, the pressure levels descend until 2 A.M. Figure 5.6 shows the *pPP* over 24 hours. The *PPamp* was higher ($p = 0.007$) for men (1.40 ± 0.13) than for women (1.33 ± 0.11).

There was no significant difference for the P_f and P_b, however there was a highly significant difference ($p < 0.001$) for the *RM* (men: $58.70 \pm 5.74\,\%$; women: $63.53 \pm 5.46\,\%$). Figure 5.8 shows the higher *RM* for women in contrast to men over 24 hours.

The *AP*, *AIx*, and *AIx@75* were $6.29 \pm 2.69\,\mathrm{mmHg}$, $17.77 \pm 6.56\,\mathrm{mmHg}$, and $13.45 \pm 6.83\,\mathrm{mmHg}$ for men, and $9.14 \pm 3.54\,\mathrm{mmHg}$, $25.25 \pm 7.59\,\mathrm{mmHg}$, and $23.50 \pm 7.62\,\mathrm{mmHg}$ for women. All three parameters are highly significantly different ($p < 0.001$) between men and women. The *AP*, *AIx*, and *AIx@75* over 24 hours are shown in figure 5.9, 5.10, and 5.11, respectively.

The *PWV* is higher in men (median: $5.91\,\mathrm{m\,s}^{-1}$; IQR: $5.24\,\mathrm{m\,s}^{-1}$ to $7.03\,\mathrm{m\,s}^{-1}$) than in women (median: $5.17\,\mathrm{m\,s}^{-1}$; IQR: $4.76\,\mathrm{m\,s}^{-1}$ to $6.61\,\mathrm{m\,s}^{-1}$) with $p = 0.032$. The results for all parameters are in table 5.2.

For all parameters the two-sample t-test (unpaired) has been used except for the *pPP* and the *PWV*. The data of the *pPP* is normal distributed but has unequal variances, hence, the Welch's t-test has been used. The mean values of the *PWV* are not normal distributed, thus the Mann-Whitney U test has been applied and in the table 5.2 the median with the IQR is stated.

Table 5.2: The parameter values classified by sex and overall. The values are mean $\pm$ SD except for the *PWV*, where the median and the interquartile range is given.

	All (#91)	**Men (#36)**	**Women (#55)**	**p**
HR (min^{-1})	70.17 ± 7.93	67.56 ± 8.57	71.88 ± 7.05	0.010
pSBP (mmHg)	116.35 ± 8.60	120.05 ± 7.43	113.93 ± 8.51	< 0.001
pDBP (mmHg)	73.04 ± 7.32	75.53 ± 7.12	71.42 ± 7.06	0.008
pMAP (mmHg)	92.89 ± 7.32	95.92 ± 6.32	90.90 ± 7.29	0.001
pPP (mmHg)	43.31 ± 6.11	44.52 ± 7.17	42.51 ± 5.23	0.153
cSBP (mmHg)	107.44 ± 8.08	109.78 ± 6.72	105.91 ± 8.57	0.025
cDBP (mmHg)	74.46 ± 7.41	77.07 ± 7.11	72.76 ± 7.15	0.006
cPP (mmHg)	32.97 ± 4.87	32.71 ± 4.73	33.14 ± 4.99	0.680
PPamp	1.36 ± 0.13	1.40 ± 0.13	1.33 ± 0.11	0.007
Pf (mmHg)	21.44 ± 3.00	21.85 ± 3.36	21.18 ± 2.73	0.295
Pb (mmHg)	13.43 ± 2.27	12.96 ± 2.01	13.73 ± 2.40	0.118
RM $(\%)$	61.62 ± 6.03	58.70 ± 5.74	63.53 ± 5.46	< 0.001
AP (mmHg)	8.01 ± 3.51	6.29 ± 2.69	9.14 ± 3.54	< 0.001
AIx $(\%)$	22.29 ± 8.05	17.77 ± 6.56	25.25 ± 7.59	< 0.001
AIx75 $(\%)$	19.52 ± 8.80	13.45 ± 6.83	23.50 ± 7.62	< 0.001
PWV (m s^{-1})	$5.59 \, (4.93 - 6.71)$	$5.91 \, (5.24 - 7.03)$	$5.17 \, (4.76 - 6.61)$	0.032
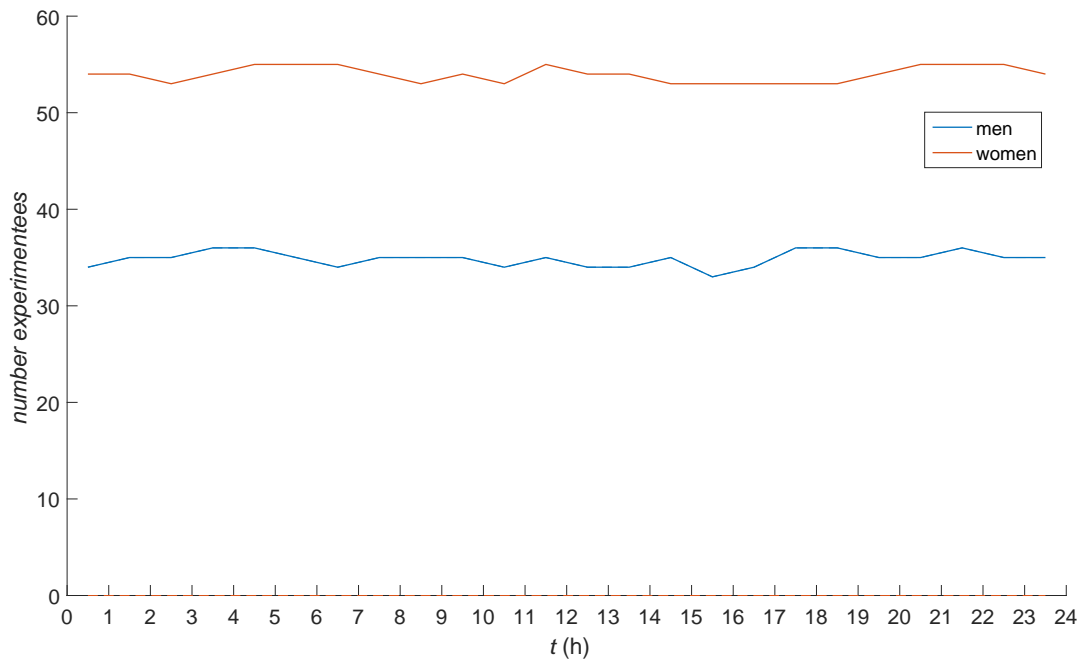
Figure 5.1: Number of experimentees over 24 hours when the data is classified by sex
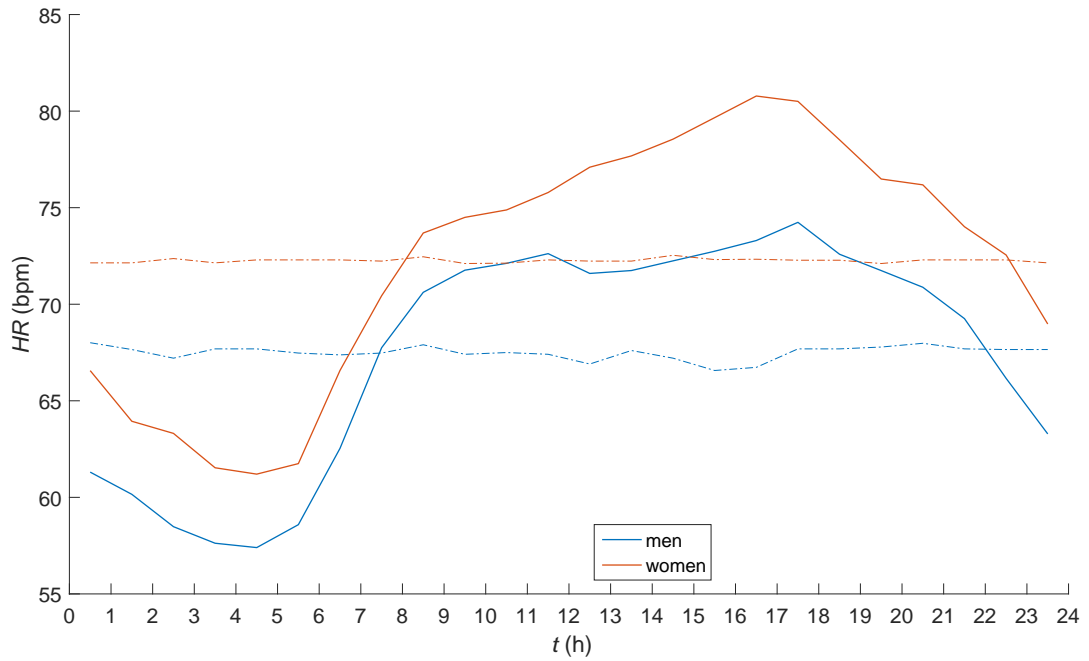
Figure 5.2: 24-hour plot of the heart rate of men and women
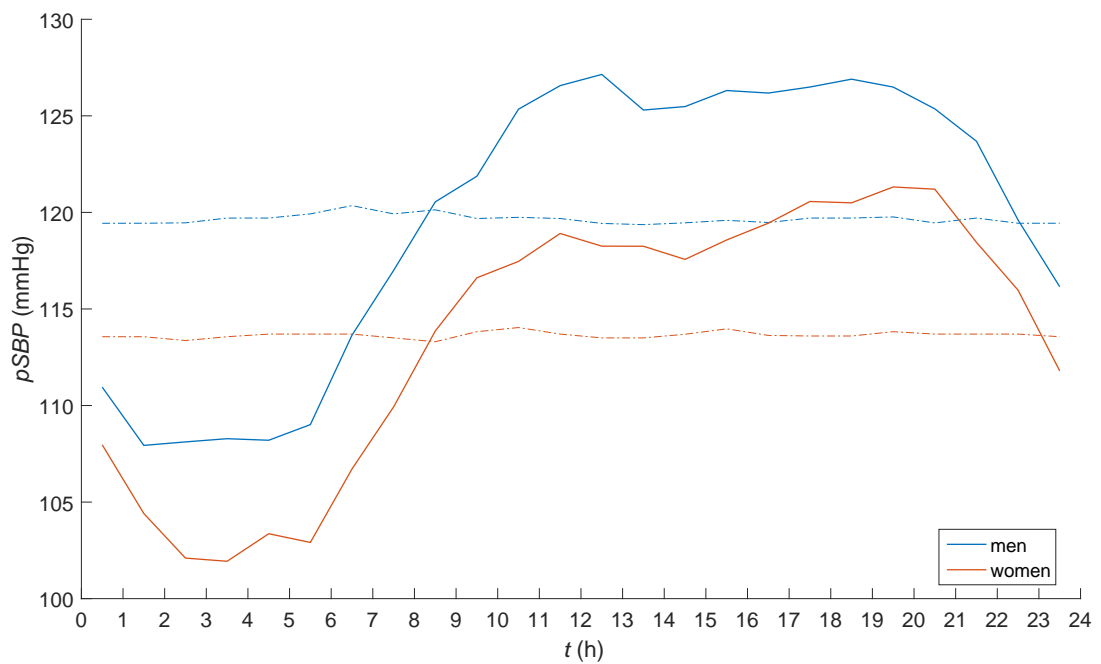
Figure 5.3: 24-hour plot of the peripheral systolic blood pressure of men and women
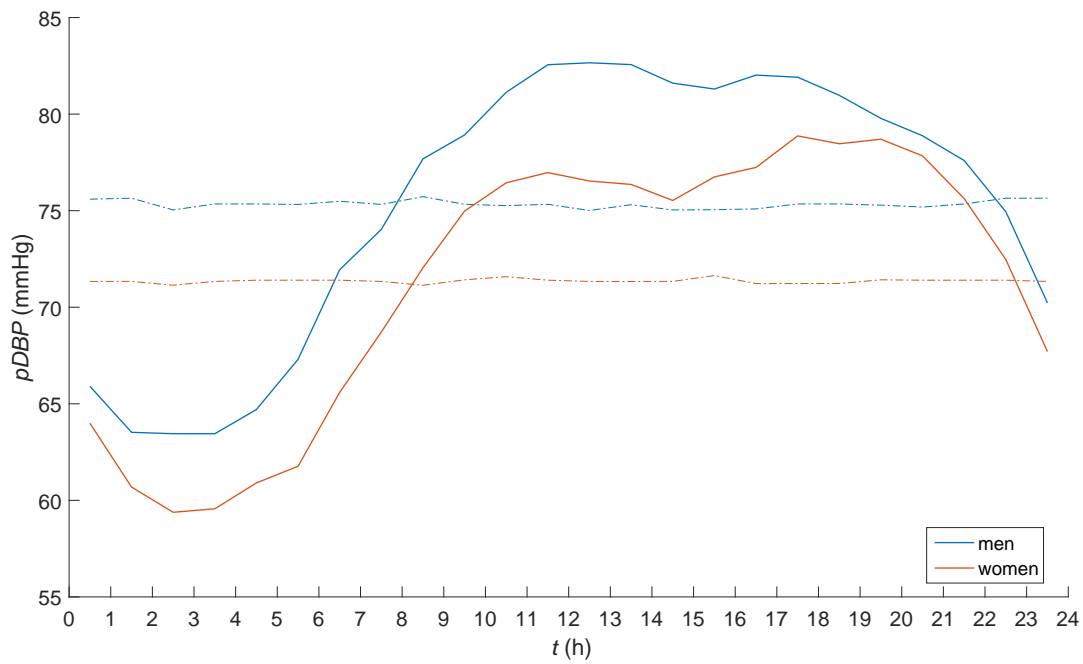
Figure 5.4: 24-hour plot of the peripheral diastolic blood pressure of men and women
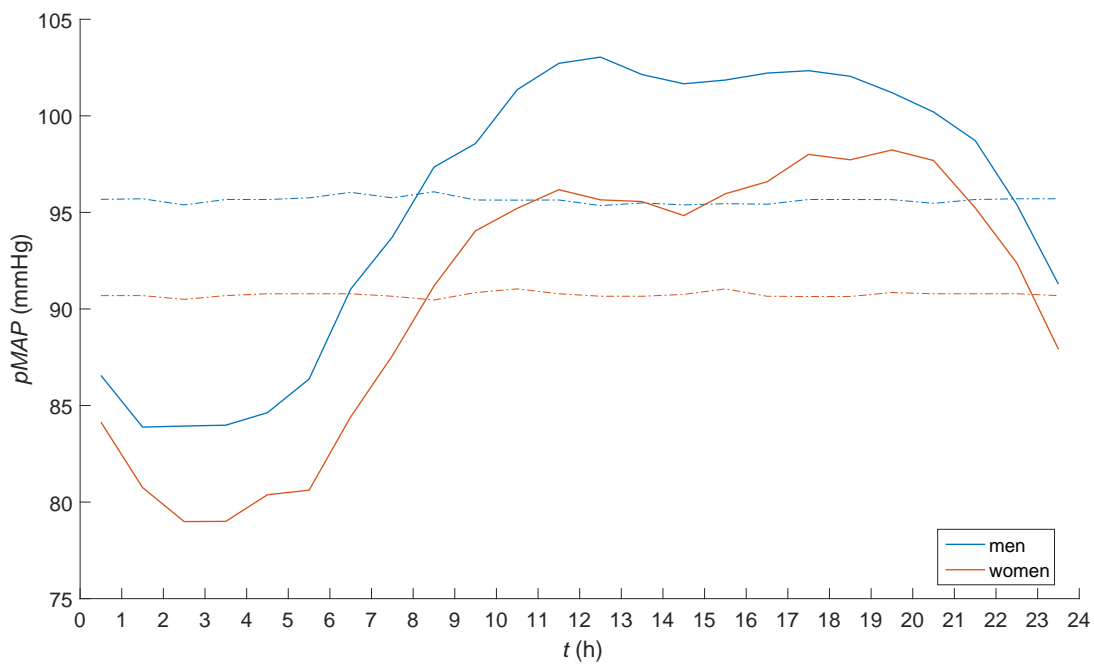
Figure 5.5: 24-hour plot of the peripheral mean arterial pressure of men and women
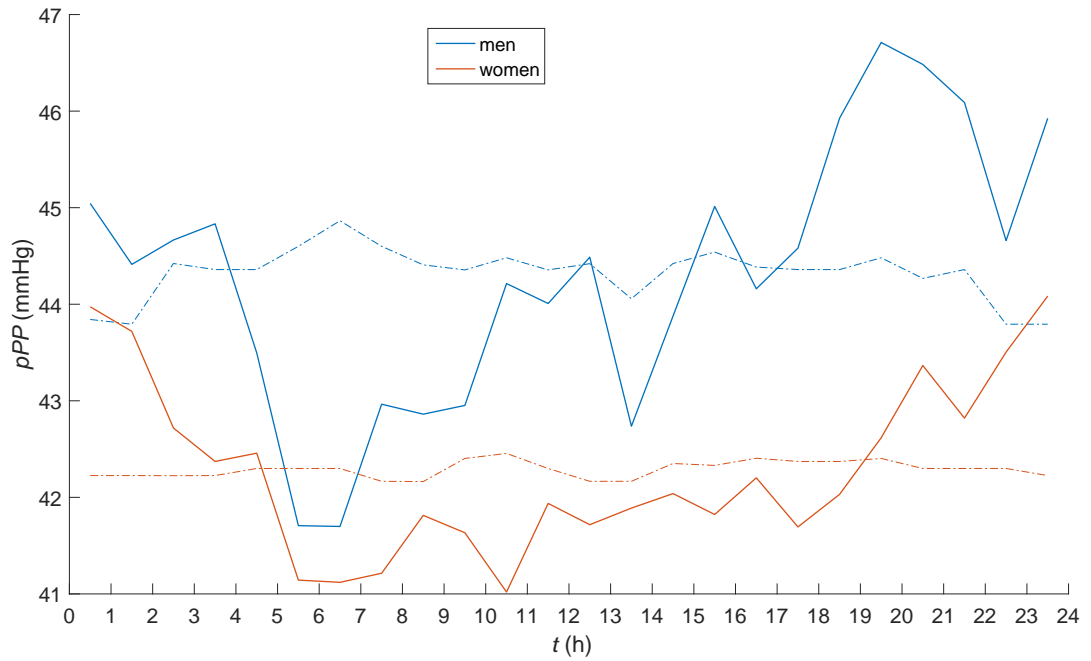
Figure 5.6: 24-hour plot of the peripheral pulse pressure of men and women
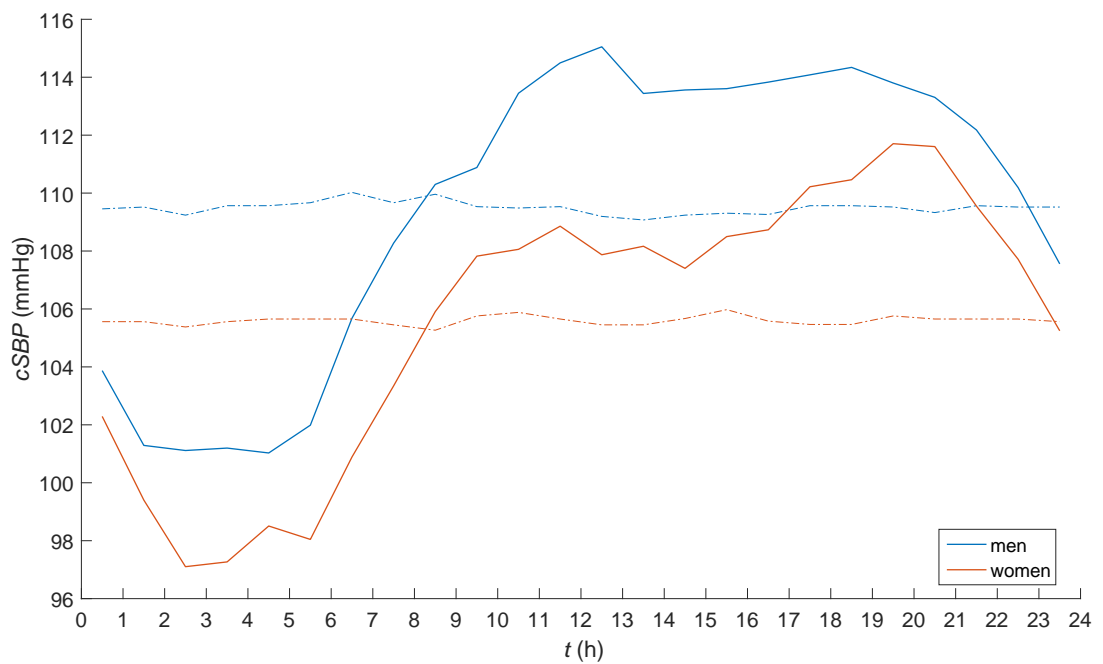
Figure 5.7: 24-hour plot of the *cSBP* of men and women
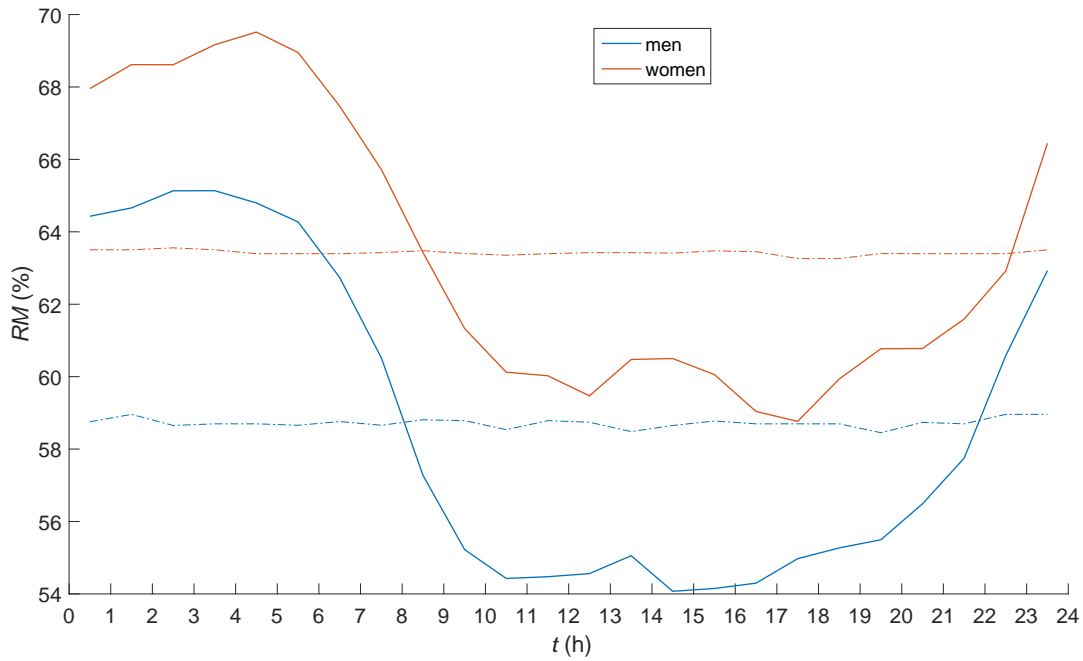
Figure 5.8: 24-hour plot of the reflection magnitude of men and women
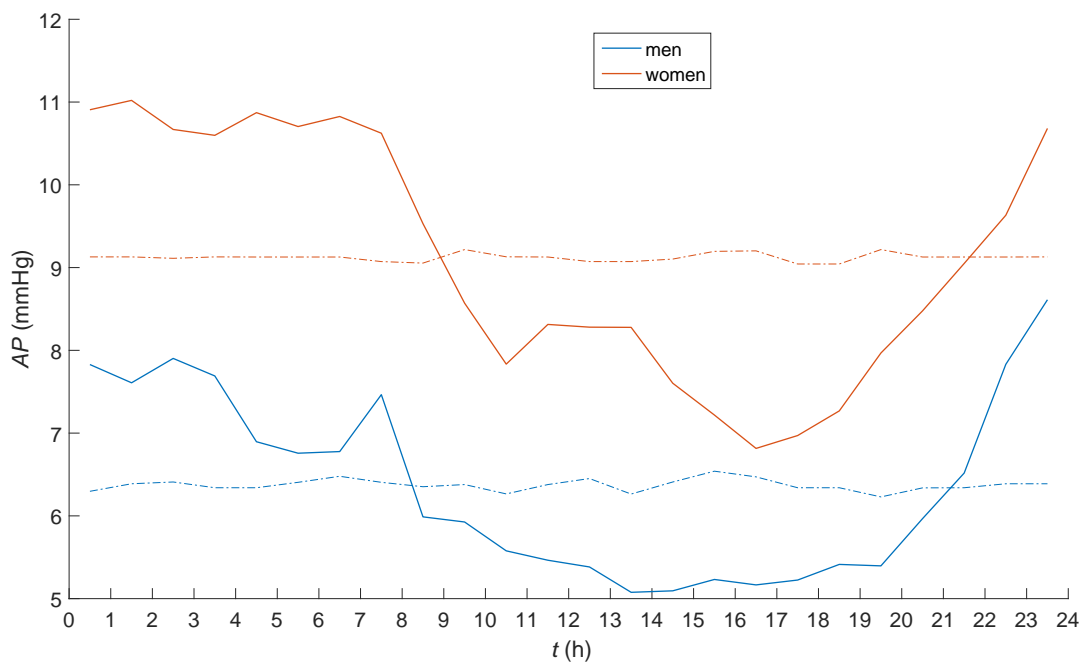
Figure 5.9: 24-hour plot of the augmentation pressure of men and women
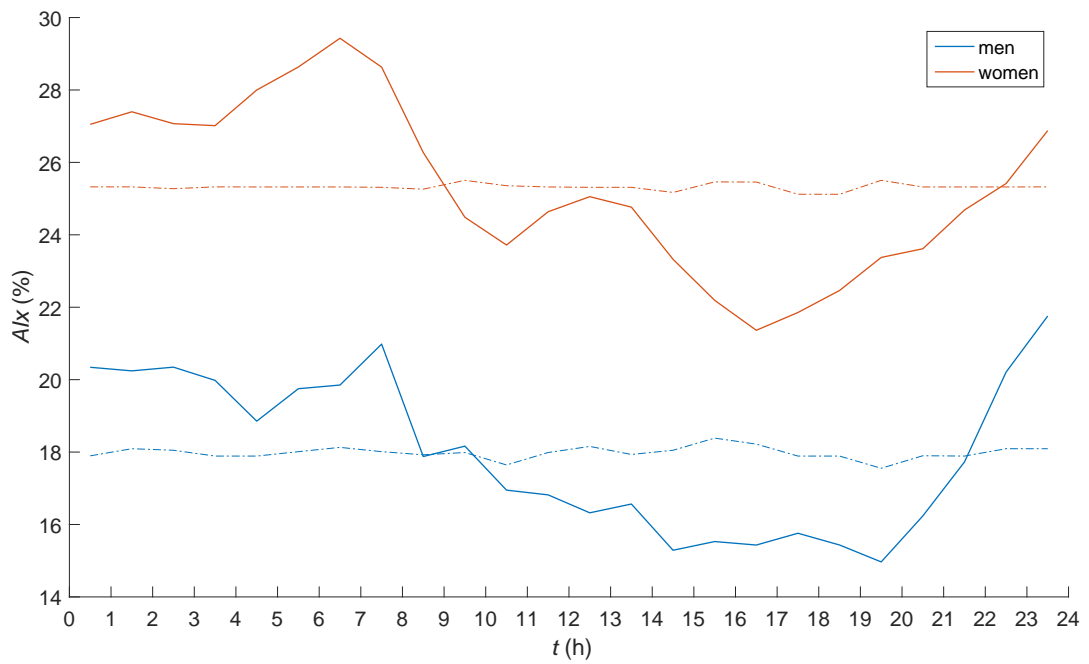
Figure 5.10: 24-hour plot of the augmentation index of men and women
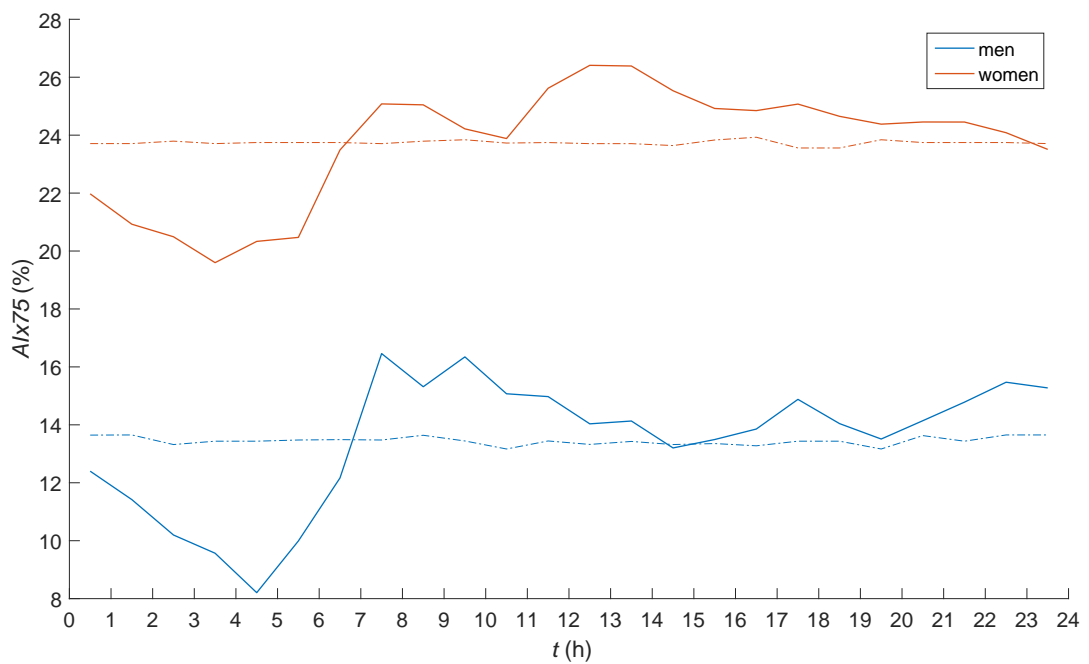
Figure 5.11: 24-hour plot of the augmentation index at $75\,\mathrm{min}^{-1}$ of men and women

5.3 Daytime vs Nighttime

5.3.1 Statistical analysis of day vs night

All parameters compared between day and night are highly significant ($p < 0.001$) different, except the *pPP* ($p = 0.748$) and the *AIx* ($p = 0.1$). The *pPP* is 43.28 ± 6.86 mmHg during the day and 43.49 ± 6.68 mmHg during the night, and the *AIx* is 20.63 ± 7.12 mmHg during the day and 24.18 ± 12.66 mmHg during the night. The day values of the *HR*, *pSBP*, *pDBP*, *pMAP*, *cSBP*, *cDBP*, *PPamp*, *AIx@75*, and *PWV* are elevated compared to the night, whereas *cPP*, P_f, P_b, *RM*, *AP*, and *AIx* are decreased.

The differences of the day and night means are normally distributed for every parameter except for the *AP* and the *AIx*, thus, the t-test for paired samples has been used to compare all parameters except these two. After the data of the *AP* and the *AIx* have been log-transformed the differences are normal distributed. Therefore, the t-test for paired samples has been executed with the log-transformed data.

Table 5.3: The parameter values divided into day and night interval, and overall. The values are mean $\pm$ SD.

	24h (#91)	Day (#91)	Night (#91)	p
HR (min^{-1})	70.17 ± 7.93	75.04 ± 9.39	61.14 ± 8.48	< 0.001
pSBP (mmHg)	116.35 ± 8.60	121.70 ± 9.51	105.75 ± 10.33	< 0.001
pDBP (mmHg)	73.04 ± 7.32	78.43 ± 8.25	62.27 ± 7.45	< 0.001
pMAP (mmHg)	92.89 ± 7.32	98.25 ± 8.16	82.20 ± 8.21	< 0.001
pPP (mmHg)	43.31 ± 6.11	43.28 ± 6.86	43.49 ± 6.68	0.748
cSBP (mmHg)	107.44 ± 8.08	110.97 ± 9.13	99.89 ± 9.80	< 0.001
cDBP (mmHg)	74.46 ± 7.41	80.09 ± 8.34	63.30 ± 7.59	< 0.001
cPP (mmHg)	32.97 ± 4.87	30.89 ± 5.49	36.57 ± 6.08	< 0.001
PPamp	1.36 ± 0.13	1.44 ± 0.16	1.22 ± 0.14	< 0.001
Pf (mmHg)	21.44 ± 3.00	20.61 ± 3.28	22.91 ± 3.71	< 0.001
Pb (mmHg)	13.43 ± 2.27	12.23 ± 2.53	15.47 ± 2.86	< 0.001
RM (%)	61.62 ± 6.03	58.40 ± 6.75	67.01 ± 6.85	< 0.001
AP (mmHg)	8.01 ± 3.51	6.97 ± 3.10	9.33 ± 5.25	< 0.001
AIx (%)	22.29 ± 8.05	20.63 ± 7.12	24.18 ± 12.66	0.100
AIx75 (%)	19.52 ± 8.80	20.73 ± 9.11	16.07 ± 12.95	< 0.001
PWV ($\mathrm{m\,s}^{-1}$)	6.00 ± 1.35	6.13 ± 1.38	5.73 ± 1.33	< 0.001

5.3.2 Day and night over age

The strongest correlation found is the increasing *PWV* with age, both for the day ($R = 0.967$, CI 0.951 to 0.978) and night interval ($R = 0.950$, CI 0.925 to 0.967) as shown in figure 5.23. There is a high negative correlation for the *PPamp* for the day ($R = -0.532$, CI -0.665 to -0.366), but no significant correlation for the night interval ($R = -0.14$, CI -0.336 to 0.068). The *PPamp* is shown in figure 5.18. The day and night values of the *PPamp* are getting closer with age and the difference is decreasing. The *cPP* has a similar behaviour, shown in figure 5.17. The difference between day and night is vanishing over age with a positive correlation for the day interval ($R = 0.316$, CI 0.118 to 0.490) and no significant correlation for the night interval ($R = -0.076$, CI -0.277 to 0.132). The *RM*, *AP*, and *AIx* have a high correlation coefficient during the day ($R = 0.414$, CI 0.228 to 0.571; $R = 0.416$, CI 0.229 to 0.573; $R = 0.388$, CI 0.198 to 0.550) as well as for the night ($R = 0.470$, CI 0.292 to 0.616; $R = 0.426$, CI 0.242 to 0.581; $R = 0.488$, CI 0.313 to 0.631). The *RM*, *AP*, and *AP* are displayed in figure 5.19, 5.20, and 5.21, respectively. The *AIx@75* has a good correlation at night ($R = 0.488$, CI 0.313 to 0.630) but not during the day ($R = 0.148$, CI -0.060 to 0.344). The *AIx@75* is shown in figure 5.22. The *HR* negatively correlates with age during the day ($R = -0.225$, CI -0.412 to -0.020) but it does not correlate during the night ($R = 0.054$, CI -0.153 to 0.257), as it can be seen in figure 5.12. The *pSBP*, *pDBP*, *cSBP*, and *cDBP* are shown in figure 5.13, 5.14, 5.15, and 5.16, respectively. For further details see table 5.3. For further details see table 5.4.

Table 5.4: Pearson's correlation coefficient R between age and the day interval, and age and the night interval with the 95 % CI.

	R day	CI		R night	CI	
		Lower	Upper		Lower	Upper
HR (min^{-1})	-0.225	-0.412	-0.020	0.054	-0.153	0.257
pSBP (mmHg)	0.196	-0.010	0.387	0.149	-0.059	0.344
pDBP (mmHg)	0.214	0.008	0.402	0.328	0.131	0.501
pMAP (mmHg)	0.221	0.015	0.408	0.247	0.043	0.431
pPP (mmHg)	0.015	-0.191	0.221	-0.136	-0.333	0.072
cSBP (mmHg)	0.376	0.185	0.540	0.194	-0.012	0.385
cDBP (mmHg)	0.205	-0.001	0.394	0.312	0.113	0.486
cPP (mmHg)	0.316	0.118	0.490	-0.076	-0.277	0.132
PPamp	-0.532	-0.665	-0.366	-0.140	-0.336	0.068
Pf (mmHg)	0.164	-0.043	0.358	-0.221	-0.408	-0.015
Pb (mmHg)	0.358	0.164	0.525	0.048	-0.159	0.252
RM (%)	0.414	0.228	0.571	0.470	0.292	0.616
AP (mmHg)	0.416	0.229	0.573	0.426	0.242	0.581
AIx (%)	0.388	0.198	0.550	0.488	0.313	0.631
AIx75 (%)	0.148	-0.060	0.344	0.488	0.313	0.630
PWV ($\mathrm{m\,s}^{-1}$)	0.967	0.951	0.978	0.950	0.925	0.967
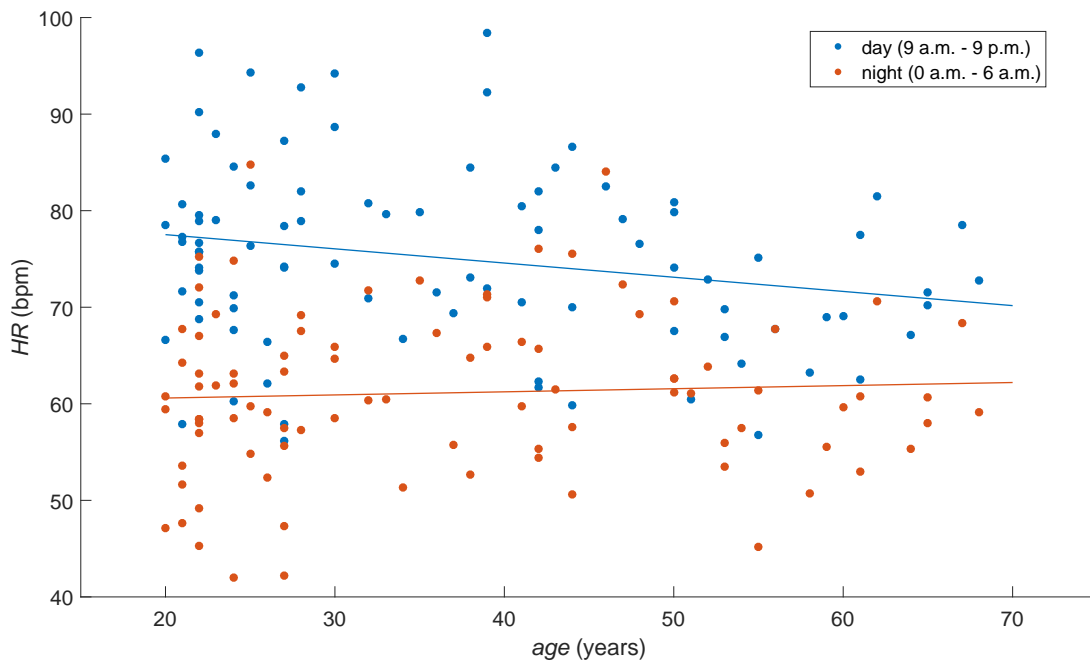
Figure 5.12: Scatter-plot of the heart rate day and night values over age
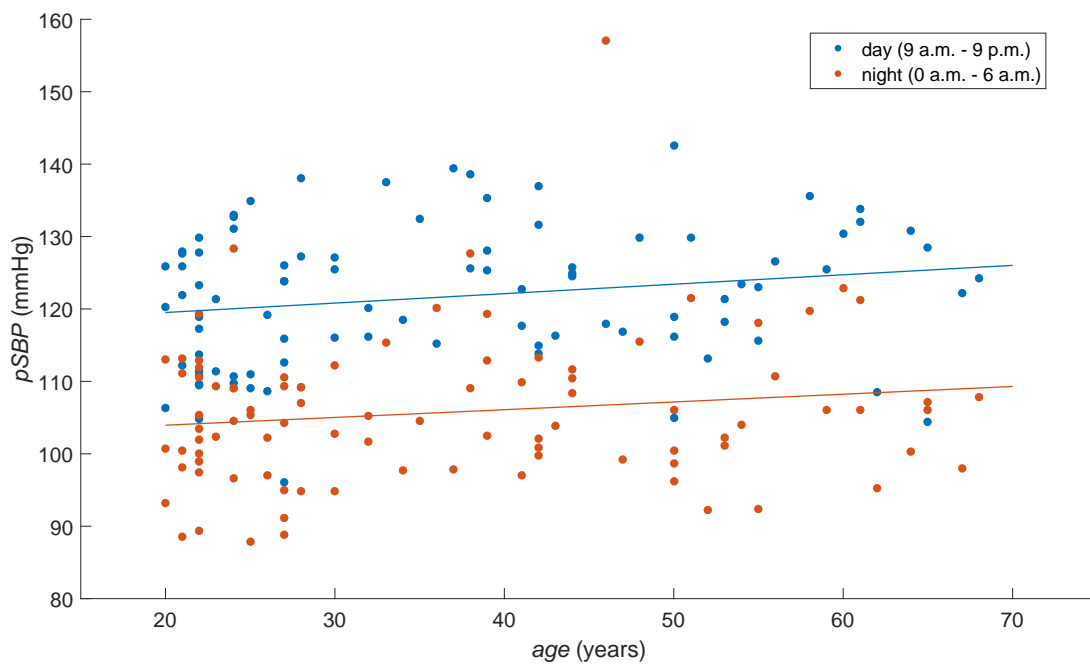
Figure 5.13: Scatter-plot of the peripheral systolic blood pressure day and night values over age
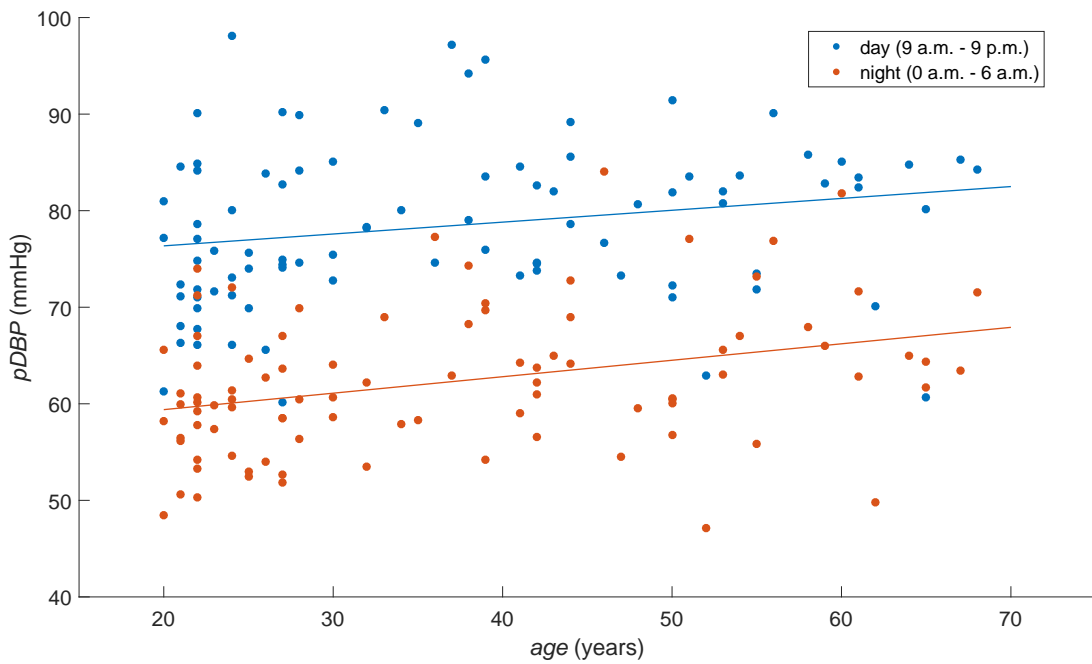
Figure 5.14: Scatter-plot of the *pDBP* day and night values over age
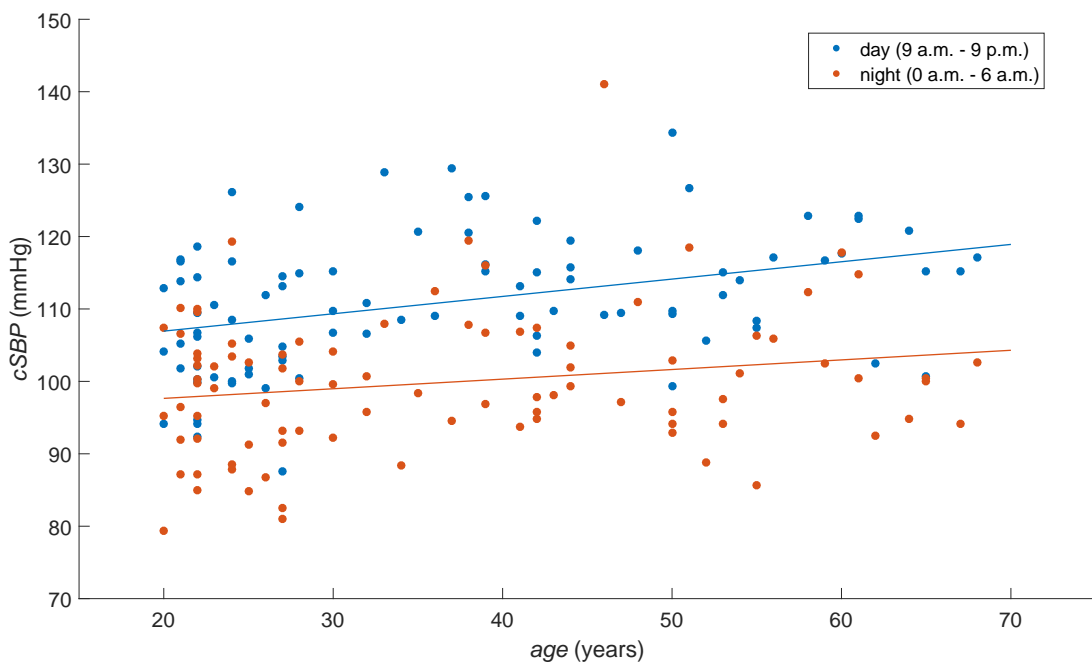
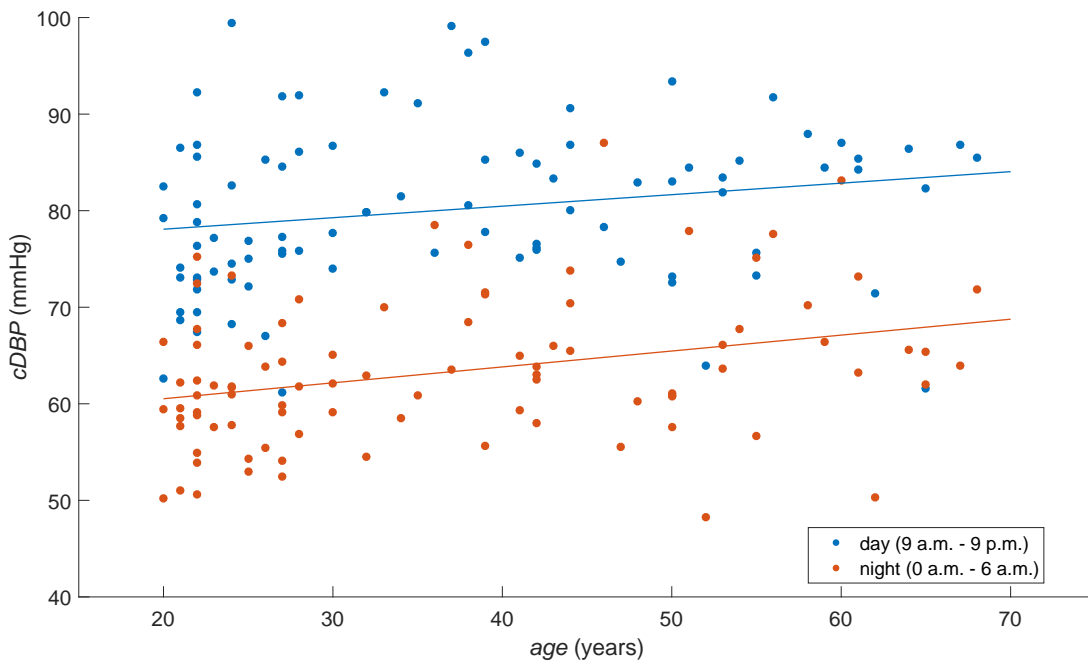**Figure 5.15:** Scatter-plot of the central systolic blood pressure day and night values over age

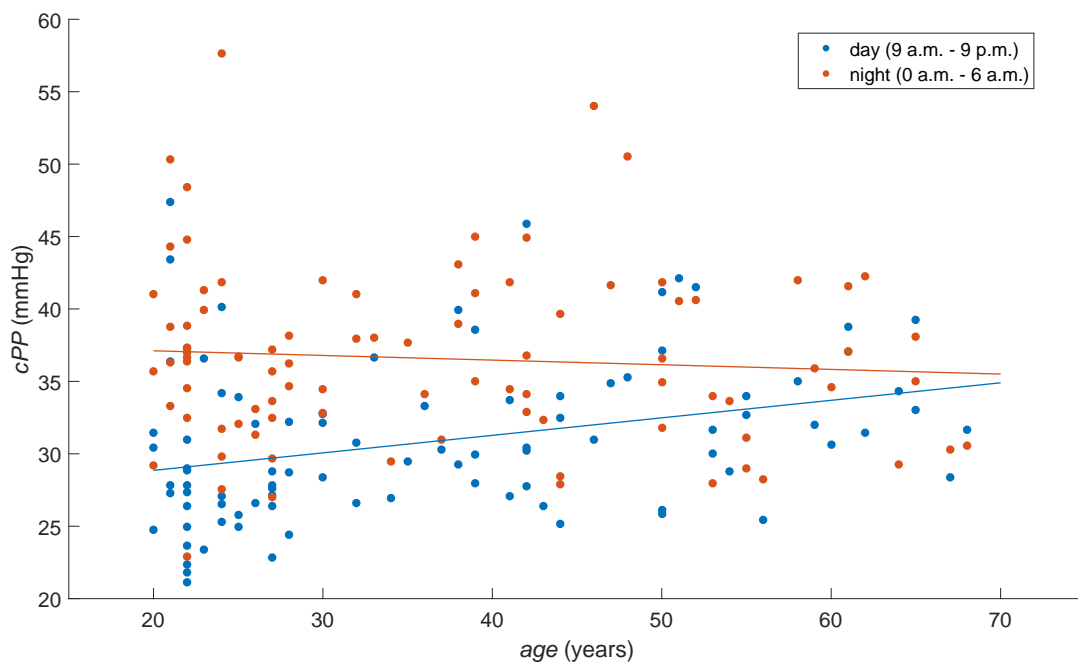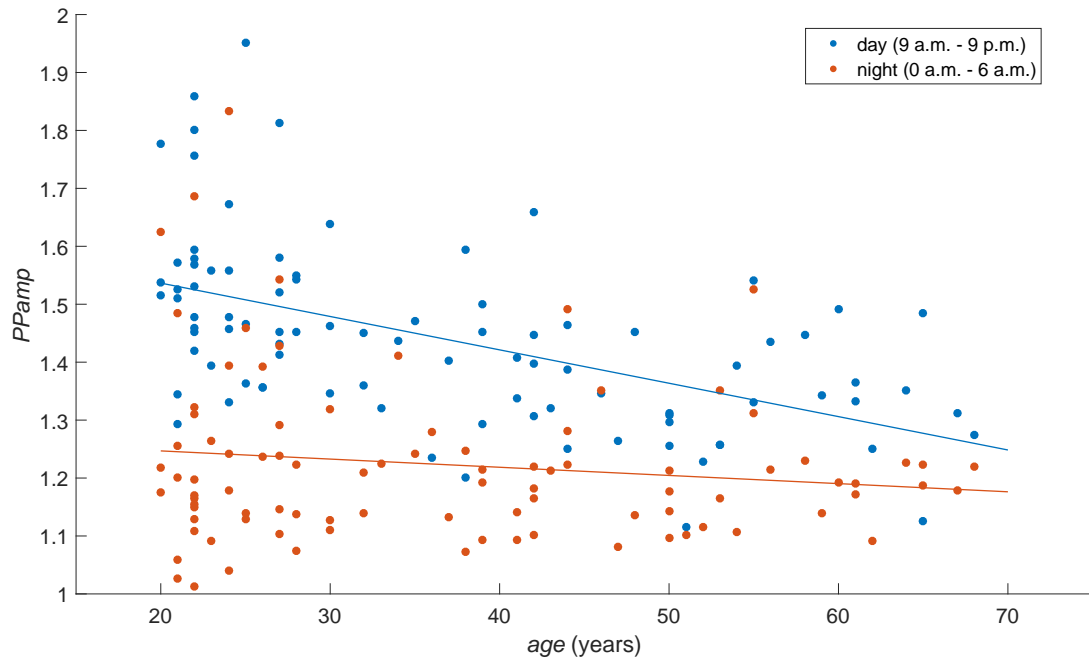**Figure 5.16:** Scatter-plot of the central diastolic blood pressure day and night values over age

Figure 5.17: Scatter-plot of the central pulse pressure day and night values over age

Figure 5.18: Scatter-plot of the pulse pressure amplification day and night values over age
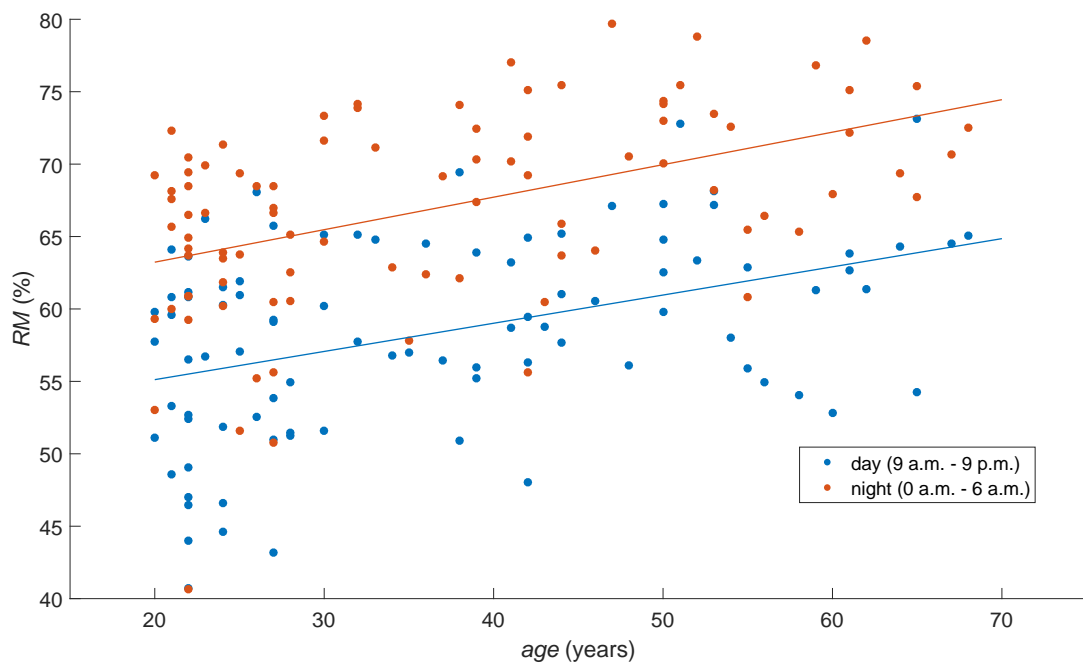
Figure 5.19: Scatter-plot of the reflection magnitude day and night values over age
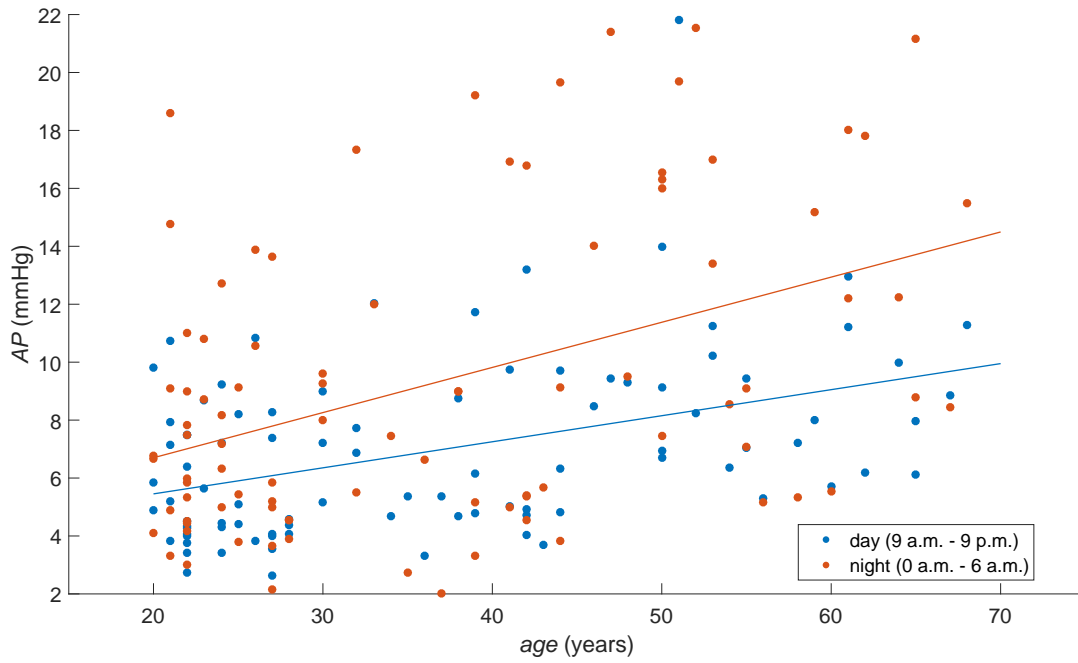
Figure 5.20: Scatter-plot of the augmentation pressure day and night values over age
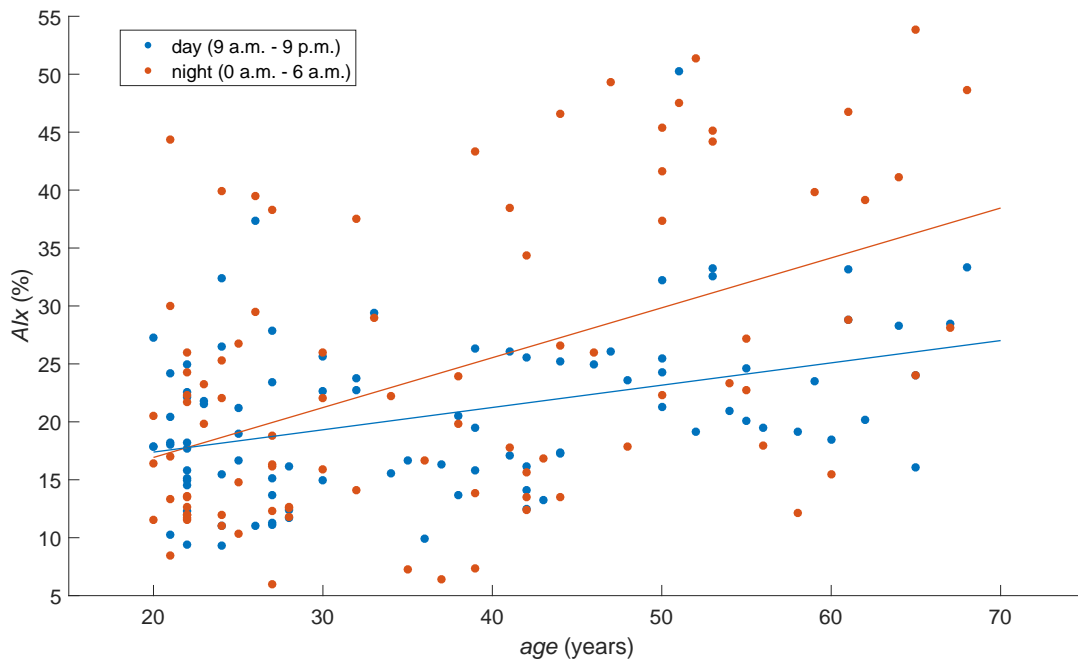
Figure 5.21: Scatter-plot of the augmentation index day and night values over age
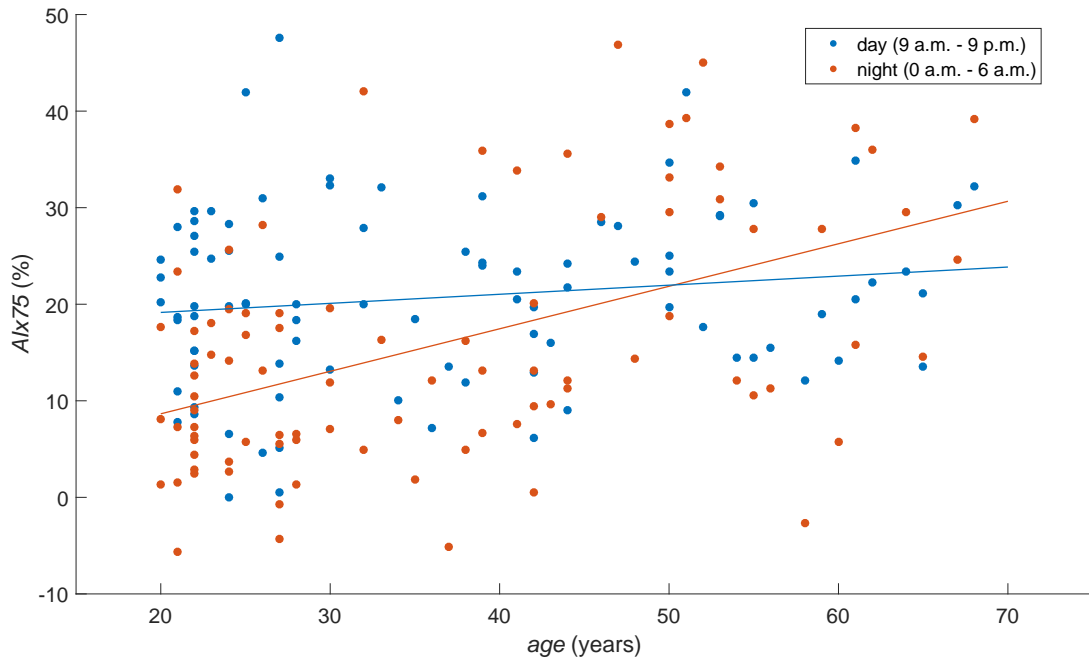
Figure 5.22: Scatter-plot of the augmentation index at $75\,\mathrm{min}^{-1}$ day and night values over age
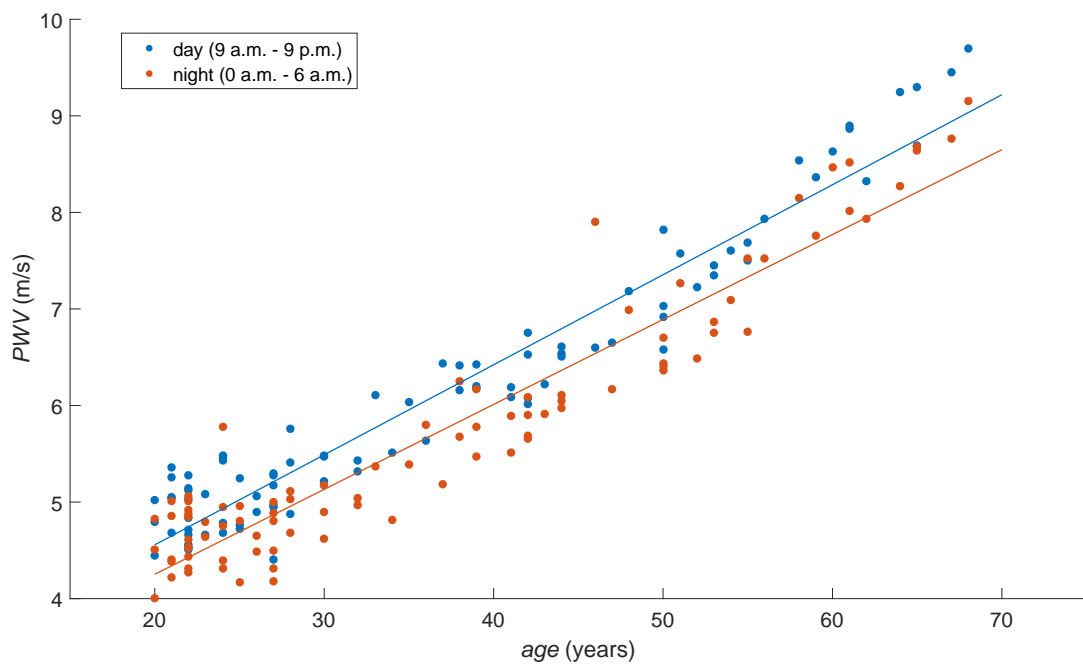
Figure 5.23: Scatter-plot of the pulse wave velocity day and night values over age

5.4 Age-related Differences

For all parameters the three age groups are not equal except for pulse pressures *cPP* (p = 0.135) and *pPP* (p = 0.930), and the P_{f} (p = 0.923). The only parameter where according to the post-hoc analysis all three groups differ significantly from each other is the *PWV* (young: $4.88 \pm 0.30\,\mathrm{m\,s^{-1}}$, middle: $5.99 \pm 0.51\,\mathrm{m\,s^{-1}}$, old: $7.95 \pm 0.86\,\mathrm{m\,s^{-1}}$). The diurnal behaviour of the *PWV* is shown in figure 5.33. The *PWV* does not show a high dynamic over 24 hours with the difference between the maximum, which is during the day, and minimum, which is during the night, per age group is lower than $1\,\mathrm{m\,s^{-1}}$. The P_{b}, *RM*, *AP*, *AIx*, and *AIx@75* show the same tendency as the *PWV* and increase with age, although the post-hoc analysis does not state a significant different between all three groups. The *AP*, *AIx*, and *AIx@75* over 24 hours classified by age are shown in figure 5.30, 5.31, and 5.32, respectively. The *AP* is highest during the night and reaches its minimum value at the late afternoon around 5 P.M. The difference between highest and lowest value over 24 hours increases with age. For the young, middle-aged, and old group the difference is about $3\,\mathrm{mmHg}$, $5\,\mathrm{mmHg}$, and $6\,\mathrm{mmHg}$, respectively. The *AIx* of the young group shows only little changes over 24 hours whereas the dynamic becomes higher with age. The old group has a high dynamic with its maximum value at 5 A.M. and its minimum value at 6 P.M. The *AIx@75* has its highest dynamic for the young group with a clear minimum at 4 A.M. The 3 age groups differ clearly during the night but during the day the difference decreases with the 3 age groups being nearly equal at 7 P.M. The *PPamp* decreases over age, as shown in figure 5.29. It can be seen that from 10 A.M. till 8 P.M. the *PPamp* has a plateau for all 3 age groups. The levels of the plateaus differ between the age groups. From 1 A.M. till 5 A.M. the three age groups reach there minimum value with nearly no difference between the age groups. The *HR*, *pSBP*, *pDBP*, *pMAP*, and *cDBP* are highest in the middle-aged group. The behaviour over 24 hours of the *HR*, *pSBP*, and *pDBP* is displayed in figure 5.25, 5.26, and 5.27, respectively. The *HR* reaches its minimum for all 3 age groups at 4 A.M. During the night from 1 A.M. till 7 A.M. the young and old group are equal. From 6 A.M. on till 10 A.M. there is a steep rise of the *HR* for all age groups. After that there is a plateau for all groups until 6 P.M. From 1 P.M. to 11 P.M. the young and middle-aged group are equal. The *pSBP* has a minimum plateau from 1 A.M. till 6 A.M. for all age groups. After that the *pSBP* is increasing and reaches a plateau from 11 A.M. till 8 P.M. Then the *pSBP* is decreasing until 1 A.M. The *pDBP* shows the same diurnal behaviour as the *pSBP*. The curves of the *pDBP* for the middle-aged and old group are nearly the same except for a dip of the old group between 3 P.M. and 5 P.M. For the *cSBP*, shown in figure 5.28, the young group differs significantly form the middle-aged and old group, but no difference between the middle-aged and old group (young: $103.51 \pm 7.91\,\mathrm{mmHg}$, middle: $110.80 \pm 6.36\,\mathrm{mmHg}$, old: $110.18 \pm 7.48\,\mathrm{mmHg}$). Further details are in table 5.5.

All groups are normally distributed and all have equal variances except the groups of the *PWV* and *PPamp*, which have unequal variances. Thus, for all parameters, except these two, an ANOVA has been executed and for the post-hoc analysis the Tukey-Kramer method has been used. The *PWV* and the *PPamp* have been tested with the Welch's ANOVA and for the post-hoc analysis the Games-Howell test has been applied.

Table 5.5: The parameter values classified by age. The values are mean $\pm$ SD. If the null hypothesis, that all groups are equal, is discarded on a significance level of $\alpha = 5\,\%$, a post-hoc analysis is performed. In the column post-hoc the groups are stated, which are different: y = young group, m = middle-aged group, o = old group

	20-29 (#40)	30-49 (#28)	50-69 (#23)	p	post-hoc
HR (min^{-1})	69.80 ± 7.83	73.45 ± 8.26	66.82 ± 6.25	0.010	m-o
pSBP (mmHg)	113.63 ± 8.97	119.17 ± 6.88	117.65 ± 8.74	0.021	y-m
pDBP (mmHg)	70.22 ± 7.18	75.66 ± 6.13	74.76 ± 7.45	0.004	y-m, y-o
pMAP (mmHg)	90.11 ± 7.17	95.61 ± 5.94	94.41 ± 7.67	0.004	y-m
pPP (mmHg)	43.41 ± 7.30	43.51 ± 5.20	42.89 ± 4.97	0.930	
cSBP (mmHg)	103.51 ± 7.91	110.80 ± 6.36	110.18 ± 7.48	< 0.001	y-m, y-o
cDBP (mmHg)	71.67 ± 7.27	77.14 ± 6.16	76.06 ± 7.64	0.005	y-m
cPP (mmHg)	31.84 ± 5.27	33.65 ± 4.50	34.12 ± 4.30	0.135	
PPamp	1.42 ± 0.14	1.33 ± 0.09	1.29 ± 0.09	< 0.001	y-m, y-o
Pf (mmHg)	21.32 ± 3.53	21.61 ± 2.67	21.46 ± 2.41	0.923	
Pb (mmHg)	12.68 ± 2.29	13.81 ± 2.12	14.24 ± 2.10	0.016	y-o
RM $(\%)$	58.49 ± 5.81	62.95 ± 4.75	65.45 ± 5.09	< 0.001	y-m, y-o
AP (mmHg)	6.43 ± 2.50	8.02 ± 3.49	10.75 ± 3.45	< 0.001	y-o, m-o
AIx $(\%)$	18.99 ± 6.51	21.19 ± 6.87	29.37 ± 7.64	< 0.001	y-o, m-o
AIx75 $(\%)$	16.46 ± 8.21	19.56 ± 8.08	24.82 ± 8.40	< 0.001	y-o
PWV $(\mathrm{m\,s}^{-1})$	4.88 ± 0.30	5.99 ± 0.51	7.95 ± 0.86	< 0.001	y-m, y-o, m-o
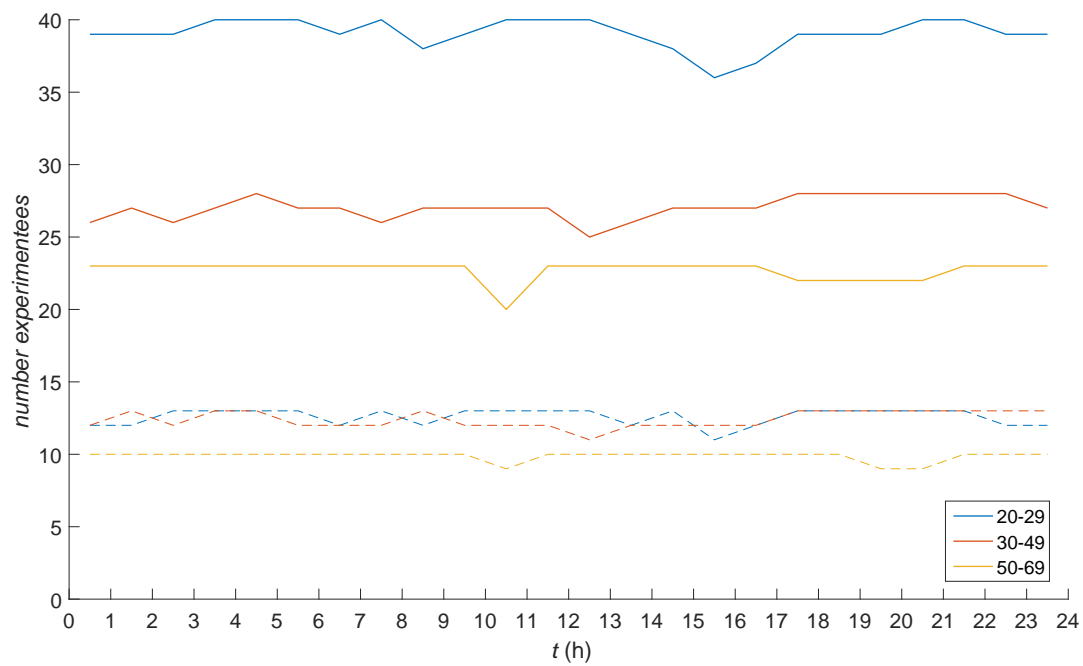
Figure 5.24: Number of experimentees over 24 hours of the 3 age groups. The dotted lines marking the number of men. The interval from the dotted to the solid line represents the number of women.
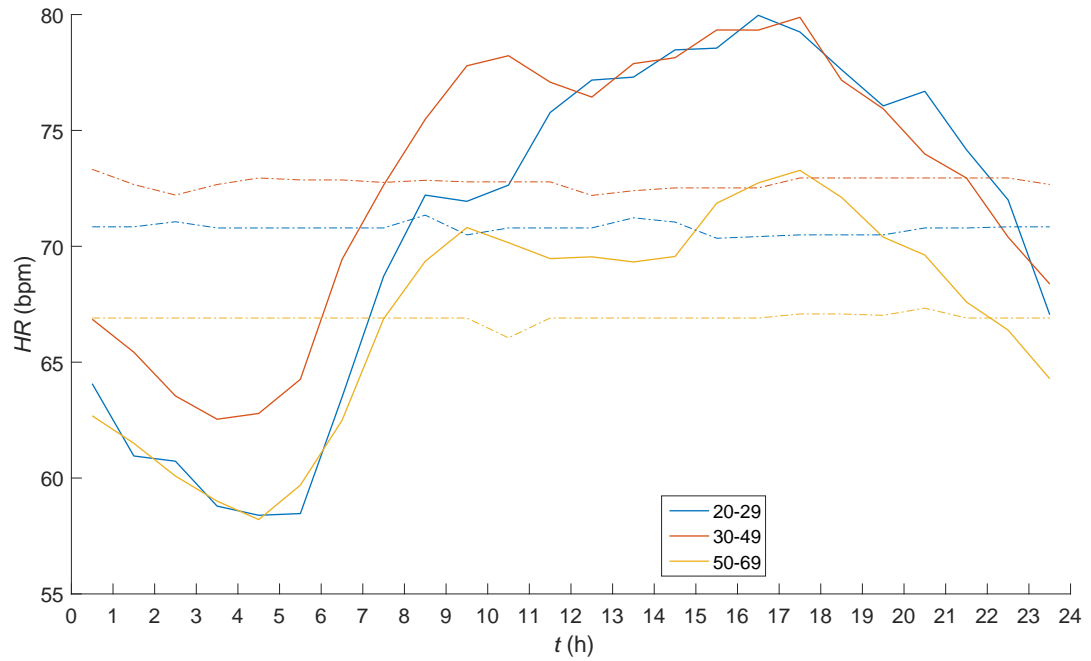
Figure 5.25: Age-dependent behaviour of the *HR* over 24 hours
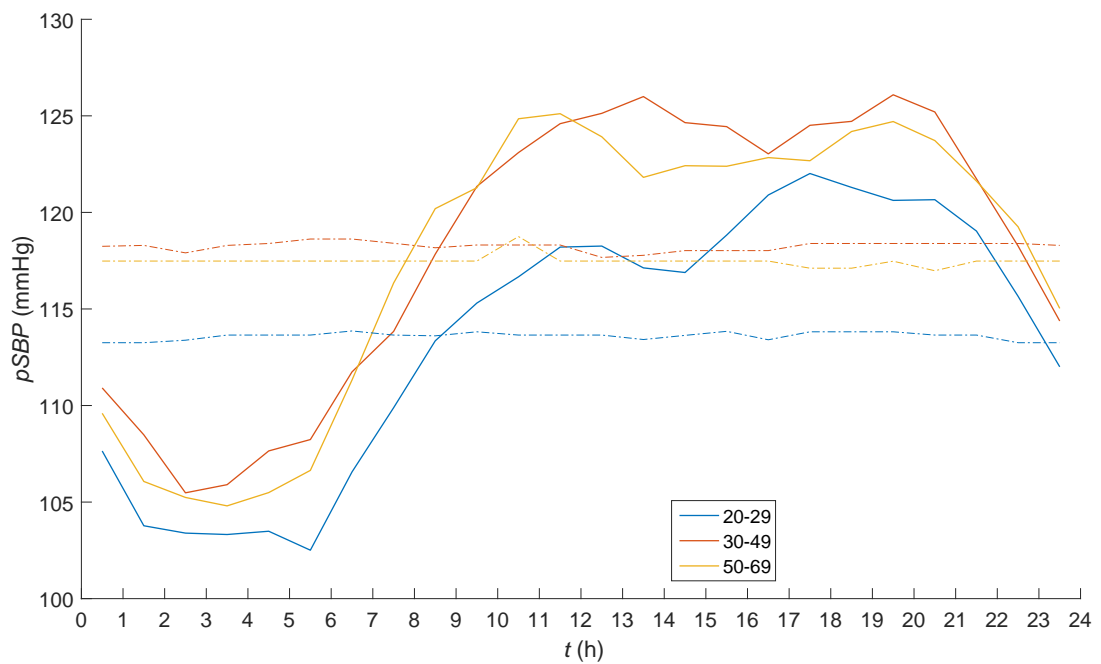
Figure 5.26: Age-dependent behaviour of the *pSBP* over 24 hours
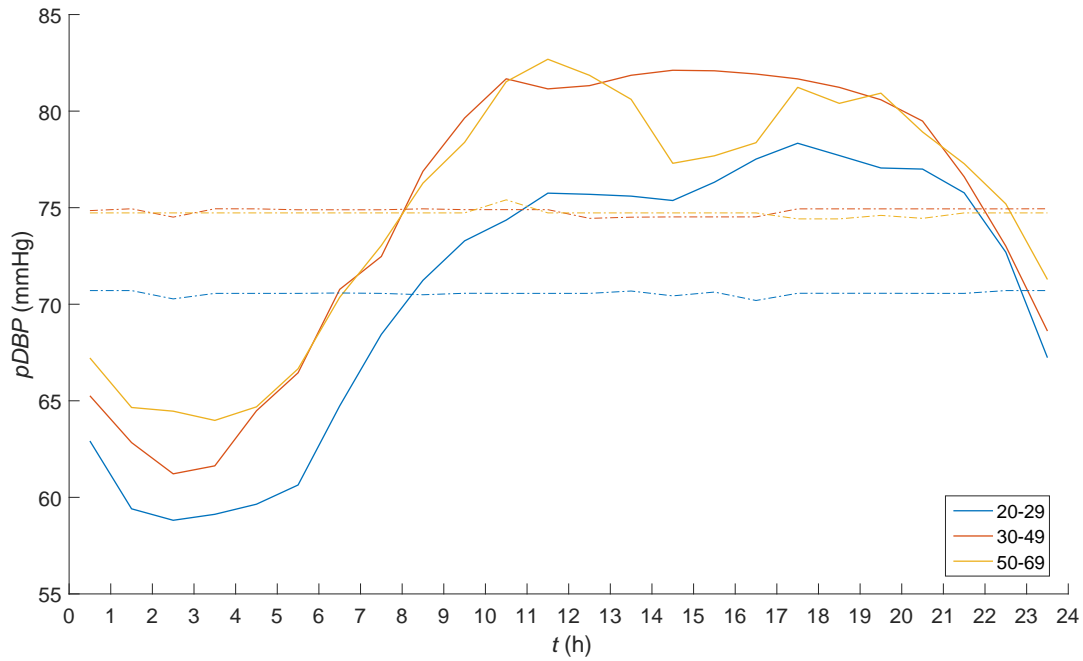
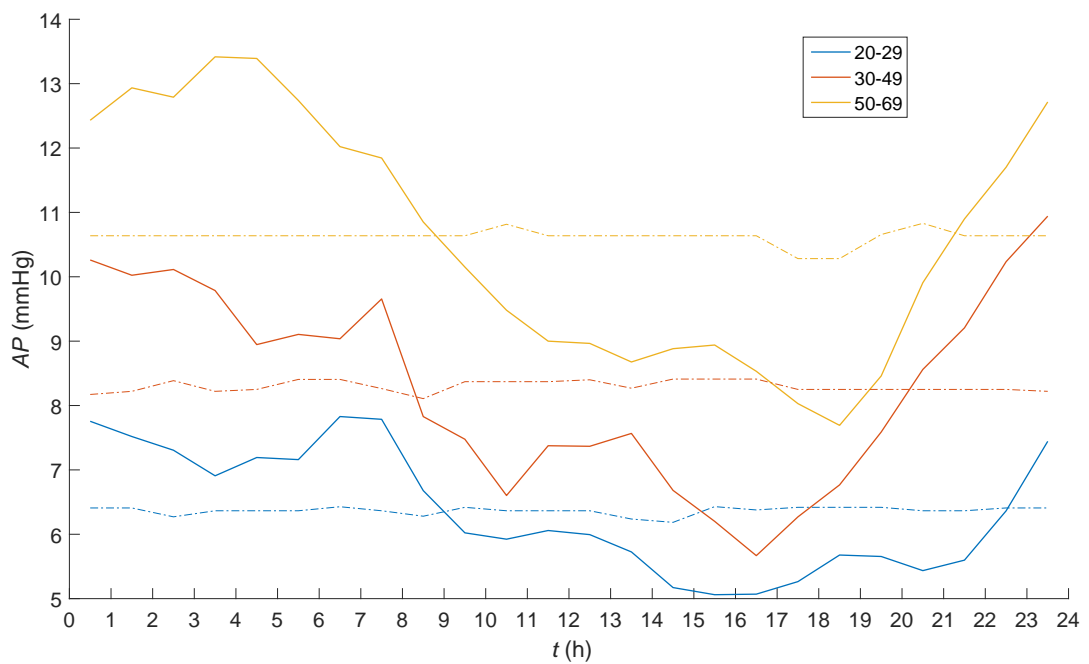**Figure 5.27:** Age-dependent behaviour of the *pDBP* over 24 hours
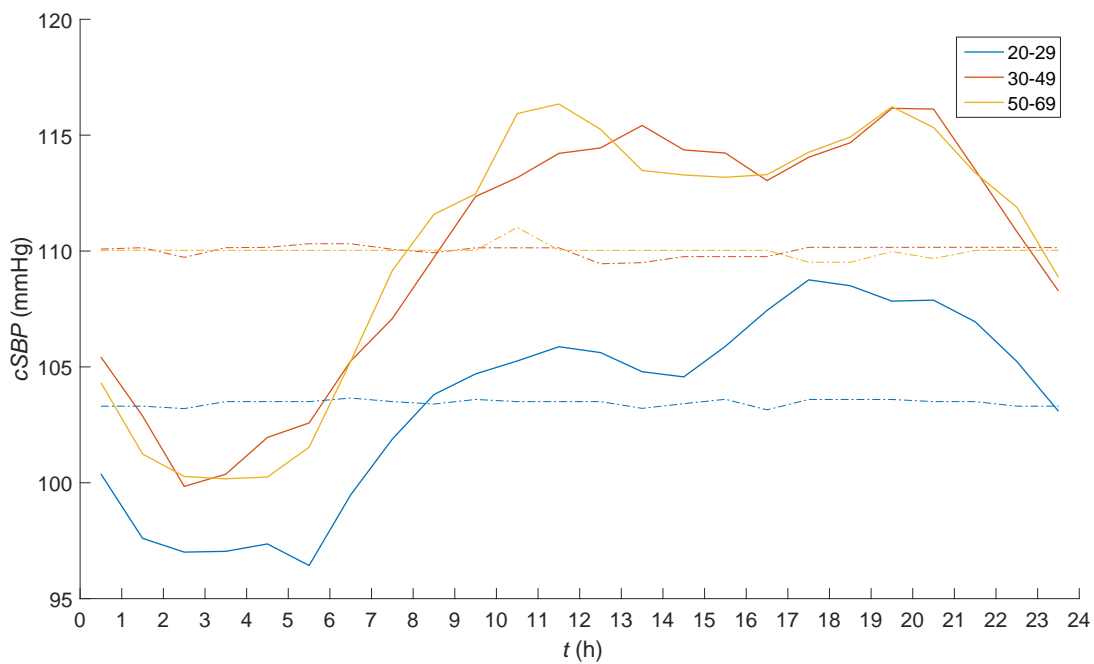
Figure 5.28: Age-dependent behaviour of the *cSBP* over 24 hours
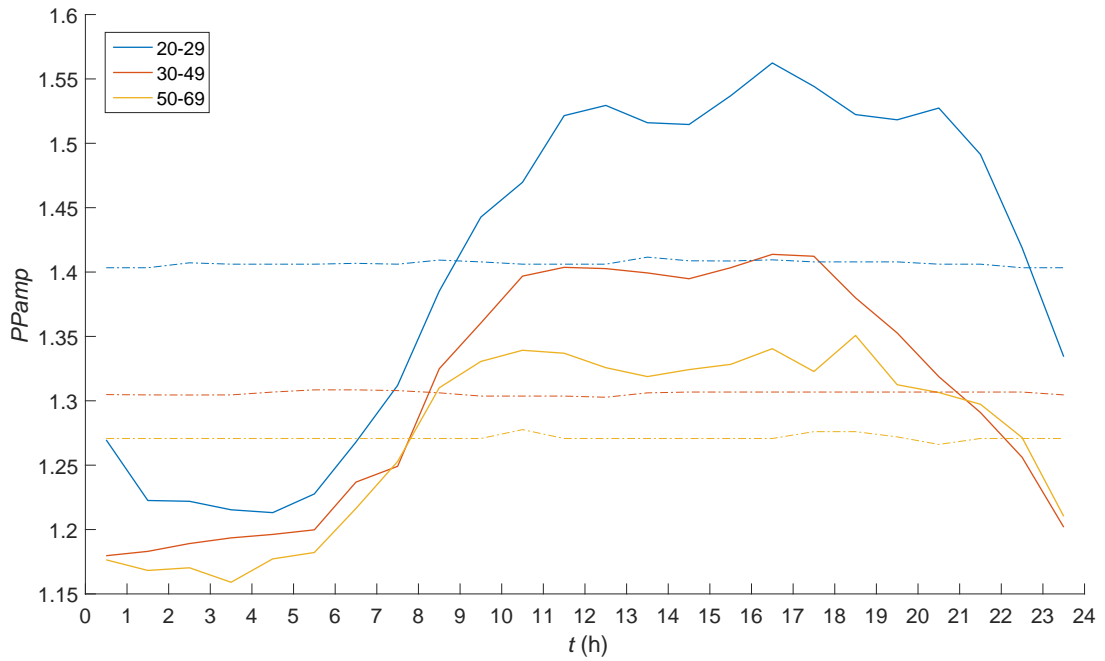
Figure 5.29: Age-dependent behaviour of the *PPamp* over 24 hours

Figure 5.30: Age-dependent behaviour of the augmentation pressure over 24 hours
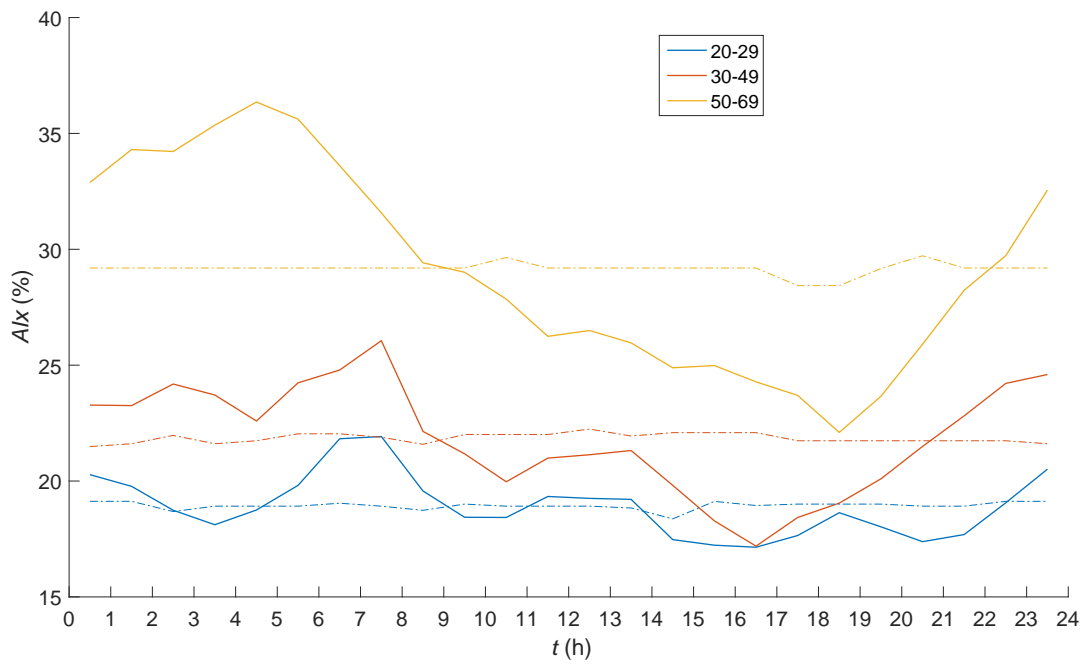
Figure 5.31: Age-dependent behaviour of the augmentation index over 24 hours
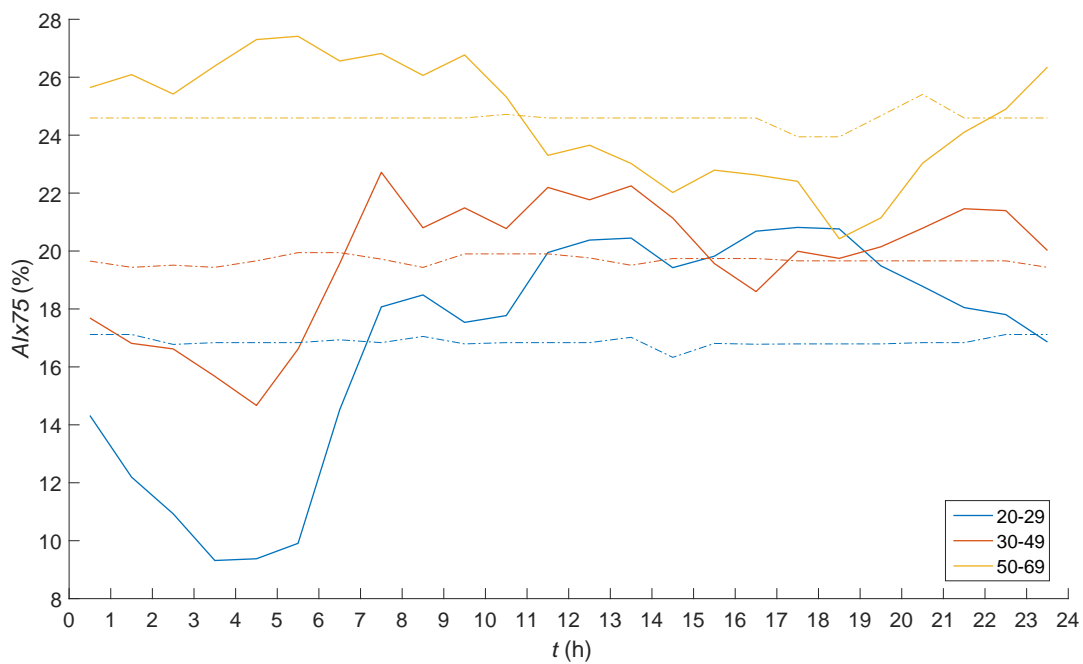
Figure 5.32: Age-dependent behaviour of the augmentation index at $75\,\mathrm{min}^{-1}$ over 24 hours
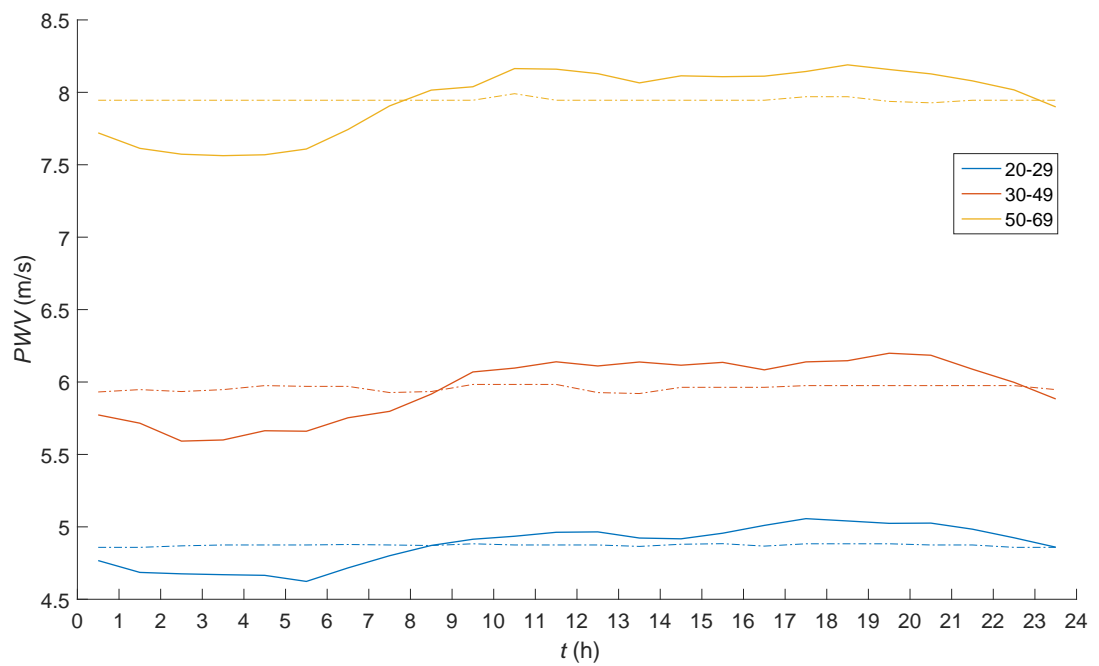
Figure 5.33: Age-dependent behaviour of the pulse wave velocity over 24 hours

CHAPTER 6

Discussion

The purpose of this thesis is to contribute to the task of establishing reference values for hemodynamic parameters. Furthermore, diurnal profiles have been investigated and statistical analysis after classifying the data. The results corresponding to the classification are discussed in this chapter as well as an outlook is given.

6.1 Men vs Women

Women compared with men have a higher heart rate and decreased blood pressure levels (*pSBP*, *pDBP*, *pMAP*, *cSBP*, *cDBP*) as well as *PPamp*, but no differences in both, peripheral and central, pulse pressure levels. The reflection magnitude is higher in women although the forward pressure wave and the backward pressure wave are not significantly different. The *AP*, *AIx*, and *AIx@75* are higher in women than in men, but the *PWV* is higher in men.

The increased *HR*, *RM*, and decreased *PPamp* agree with the results of Lieber et al. [16] and Boggia et al. [3]. Contrary to them are the differences in the blood pressure levels, which they did not observe. This can probably be explained by the study populations. Lieber et al. recruited a hypertensive cohort and Boggia et al. a random population with healthy and diseased participants mixed, whereas the cohort, which this thesis is based on, is a healthy one. Mitchell et al. [22] investigated a healthy population too and observed the same tendencies: Elevated *HR* in women, decreased BP levels and no difference for the *pPP*. Also the *AIx* was higher for women and the *PWV* decreased. Herbert et al. [12] have established reference values for a general healthy population for the *cSBP*. The tendency of higher *cSBP* in men is consistent between this thesis and Herbert et al. This could lead to the assumption, that in healthy populations there is a difference in all blood pressure levels (*pSBP*, *pDBP*, *cSBP*, *cDBP*) between men and women, but if there are medical conditions these differences vanish. Another reason could be the age of the study population. The study population of this thesis is a rather young one with especially young women, like shown in figure 4.4. The reference values for the *cSBP* of Herbert et al. [12] show the tendency that the differences between men and women are disappearing with increasing age.

Furthermore, it must be taken into account that these reference values are derived from single measurements and the values from this thesis are 24-hour mean values. The dynamic over 24 hours of the *cSBP* when classified by sex can be seen in figure 5.7.

The increased *AP*, *AIx*, and *AIx@75* in women is consistent with the findings of Torjesen et al. [42]. Torjesen et al. states that these differences in men and women could partly be explained by the forward and backward wave morphology. Another factor for the increased *AP*, *AIx*, and *AIx@75* in women could be the body height. Women are smaller than men and according to Smulyan et al. [36] have therefore a faster heart rate and an increased systolic augmentation. The elevated *PWV* of small people is not consistent with the findings in this thesis, where it is higher in men than in women, although it is not highly significant ($p = 0.032$). *PWV* is dependent on age [4], hence, one influencing factor could be that the median age of men is $7.5\,\text{years}$ higher compared to women in this cohort. Another factor of lower *PWV* but higher *AP*, *AIx*, and *AIx@75* might be explained by the fact that wave reflection is not the sole contributor to increased *cSBP* [13].

6.2 Daytime vs Nighttime

All parameters compared between day and night are highly significant different, except *pPP* and *AIx*. During the day *HR*, *pSBP*, *pDBP*, *pMAP*, *cSBP*, *cDBP*, *PPamp*, *AIx@75*, and *PWV* are elevated compared to the night, whereas *cPP*, P_f, P_b, *RM*, *AP*, and *AIx* are decreased. The nocturnal decrease in peripheral and central blood pressure levels both diastolic and systolic goes along with the findings from Boggia et al. [3]. The same accounts for the behaviour of the *PP* and *PPamp*. There is no difference of the *pPP*, but of the *cPP*. Hence, the peripheral systolic and diastolic BP decreases equally during night, whereas the *cDBP* decreases more than the *cSBP*. Since the *cPP* is elevated at night, the *PPamp* is reduced.

An interesting aspect is the inverse behaviour of the *AIx* and the *AIx@75*. The *AP* and the *AIx* are elevated during the night. Controversial to that, the *AIx@75* is higher during the day. Main factor seems to be the higher *HR* in the daytime, crucially determining the *AIx@75*. This is probably due to the significant linear inverse relationship of the *HR* and *AIx* like reported from Wilkinson et al. [54], on which the calculation of the *AIx@75* is based. Wilkinson et al. uses in his study 22 subjects with a mean age of $63\,\text{years}$ and permanent cardiac pacemakers, whereas the age of the population which this thesis is based on ranges from $20\,\text{years}$ to $68\,\text{years}$ and the cohort consists of only healthy participants. Stoner et al. [37] has examined if the *AIx* should be normalized to *HR*. Several concerns are raised with one being that the findings of Wilkinson et al. [54] are applied across all populations. It should be further investigated, if the *AIx@75* is a valid parameter for all cohorts.

One aspect which must be taken into account, when comparing day and night values, is the body position, since it can be assumed, that the experimentees are in a supine position during the night and in an upright position during the day. There are some investigations if the body position does have an effect on hemodynamic parameters. Tabara et al. [39] discovered a reduced *HR* and peripheral BP levels from sitting to supine, but an increased *pPP*. The participants have been free from any history of CVDs. Nürnberger et al. [27] reported a decreased *HR*, *pDBP*, and *cSBP* (dependent on the used device) in supine position contrary to a sitting position, but

no differences for *pSBP*, *PWV*, *AIx*, *AIx@75*, and *AP*. Tahvanainen et al. [40] investigated the difference between the supine position and a passive head-up tilt in a healthy population as well as the reproducibility of the measurements. Both systolic values, radial and aortic, have been higher in supine position as well as *cPP* and *AIx*, contrary both diastolic pressure values and *HR* have been decreased. All findings from Tahvanainen et al. are consistent with the results of the day/night evaluation except both systolic pressure values, radial and aortic, and *AIx*. It has been shown that the body position has a significant effect on hemodynamic parameters, but it is probably not the sole contributor of the day and night differences. The differences can probably also be explained with the body underlying circadian biological rhythms of organ, circulatory, and metabolic functions [41, 15].

6.3 Age-related Differences

Several BP levels are highest in the middle-aged group, which are *pSBP*, *pDBP*, *pMAP*, *cSBP*, and *cDBP*. Both *PP* levels do not change significantly over age, whereas *PPamp* decreases with age.

An interesting aspect is that the forward pressure wave does not change over age, but the backward pressure wave increases, thus, the *RM* increases too. This is probably due to changes of the reflection behaviour of the periphery. Furthermore, the *PWV* is highly significantly raising with age. This behaviour is well described [22] and does not come unexpected, since the ARC-Solver method uses age, central pressure, and aortic characteristic impedance to determine the *PWV* [25, 9]. The *PWV* and the elevated *RM* are jointly responsible for the increased *AP*, *AIx*, and *AIx@75* over age. The higher the *PWV*, the earlier returns the reflected wave, which shifts the inflection point more from late systole to early systole. In combination with the elevated P_b, the reflected wave leads to a higher *AP*. The heightened *PWV* is mostly due to increased arterial stiffness [24].

Boutouyrie and Vermeersch [4] divided the data into six age groups compared to the three of this thesis, but nevertheless *PWV* values in table 5.5 are lower than the reference values stated by Boutouyrie and Vermeersch. The mean values of this thesis for the young (20 years to 29 years), middle-aged (30 years to 49 years), and old group (50 years to 69 years) are $4.88\,\mathrm{m\,s^{-1}}$, $5.99\,\mathrm{m\,s^{-1}}$, and $7.95\,\mathrm{m\,s^{-1}}$, respectively. The mean values from Boutouyrie and Vermeersch are $6.2\,\mathrm{m\,s^{-1}}$ for under 30 years, $6.5\,\mathrm{m\,s^{-1}}$ for 30 years to 39 years, $7.2\,\mathrm{m\,s^{-1}}$ for 40 years to 49 years, $8.3\,\mathrm{m\,s^{-1}}$ for 50 years to 59 years, $10.3\,\mathrm{m\,s^{-1}}$ for 60 years to 69 years, and $10.9\,\mathrm{m\,s^{-1}}$ for 70 years and older. One reason to explain the differences could be that Boutouyrie and Vermeersch used the cf-*PWV* whereas in this thesis the aortic *PWV* is stated. Another aspect could be the fact that Boutouyrie and Vermeersch used single measurements, whereas the data in table 5.5 is based on 24-hour mean values. The *PWV* decreases during the night, which can be seen in figure 5.33 where the dynamic of the *PWV* over 24 hours is shown.

6.4 Methods for 24 hour evaluation

Boggia et al. [3] and Luzardo et al. [18] programmed the Mobil-O-Graph to make recordings every 20 minutes from 7 A.M. to 11 P.M. and every 30 minutes from 11 P.M. to 7 A.M. Further,

the record of a subject is restricted to 24 hours if they are longer and measurement quality 1 and 2 are considered. The day and night intervals are defined from 10 A.M. to 10 P.M. and 0 A.M. to 6 A.M., respectively. For the purpose of plotting, the values are averaged over 2 hours resulting in 12 values which are plotted over 24 hours. The differences to the study in Luebeck and this thesis are the recording intervals of the Mobil-O-Graph which are every 15 minutes from 8 A.M. to 11 P.M. and every 30 minutes from 11 P.M. to 8 A.M., and the day interval ranges from 9 A.M. to 9 P.M. Further, the method for the graphical representation is different with the smoothing process distinguishing between the method from Boggia et al. and Luzardo et al., and this thesis. In contrast to plotting 12 values over 24 hours in this thesis a smoothing process is used after which 24 values are plotted.

Reference values and methods are well established for single measurements, but they are new and under development for 24-hour evaluation. Different approaches will be published in future, and for use in clinical routine standardization and validation of processes must be established. An aspect is the weighting of the data not only for plotting purposes, but also for the computation of the 24-hour, day, and night mean values. Before calculating the mean values no weighting process was applied in this thesis. This could be further investigated, how the results are influenced by weighting the data beforehand.

6.5 Outlook

Progressing technologies are leading to new devices, which facilitate the recording and measurement of central hemodynamic parameters. A problem is the amount of heterogeneous methods and devices. As Boggia et al. [3] state, there is consensus that a procedure for validation of such devices should be standardized, as it is done for conventional BP measuring [28].

Still a lot of work has to be done to identify and to validate hemodynamic parameters as marker for cardiovascular diseases, nevertheless, a lot of studies have been done already and are ongoing. *PPamp* is said to be a predictor for cardiovascular mortality [1]. *AIx* is an established parameter for arterial stiffness and wave reflection assessment. But there are some investigations that it might be not as powerful as thought [11, 14]. Heim et al. [11] introduce the concept of a diastolic *AIx* with the same linkage to arterial stiffness and emphasizes the advantage towards the common systolic *AIx* of being independent of the heart rate. This might be an alternative to the *AIx@75* to overcome *HR* dependency. Moreover, Hughes et al. [14] highlights the limitations of the *AIx* contrary to the *PWV* as marker to predict cardiovascular (CV) events.

Apart from detecting pathologies it is equally important to establish reference and characteristic values of the parameters for healthy populations. The study realised in Luebeck contributes to this task as well as the data evaluation of this diploma thesis.

List of Figures

Bibliography

[1] Athanase Benetos, Frédérique Thomas, Laure Joly, et al. Pulse pressure amplification: a mechanical biomarker of cardiovascular risk. *Journal of the american college of cardiology*, 55(10):1032–1037, 2010.

[2] Yoav Ben-Shlomo, Melissa Spears, Chris Boustred, et al. Aortic pulse wave velocity improves cardiovascular event prediction: an individual participant meta-analysis of prospective observational data from 17,635 subjects. *Journal of the american college of cardiology*, 63(7):636–646, 2014.

[3] José Boggia, Leonella Luzardo, Inés Lujambio, et al. The diurnal profile of central hemodynamics in a general uruguayan population. *American journal of hypertension*, 29(6):737–746, 2016.

[4] P. Boutouyrie, S. J. Vermeersch, et al. Determinants of pulse wave velocity in healthy people and in the presence of cardiovascular risk factors: establishing normal and reference values. *European heart journal*, 31(19):2338–2350, 2010.

[5] Chen-Huan Chen, Erez Nevo, Barry Fetics, et al. Estimation of central aortic pressure waveform by mathematical transformation of radial tonometry pressure validation of generalized transfer function. *Circulation*, 95(7):1827–1836, 1997.

[6] Cmglee. A sankey diagram of the human circulatory system with approximate relative percentages of cardiac output delivered to major organ systems, drawn by cmg lee based on data at http://www.vhlab.umn.edu/atlas/physiology-tutorial/cardiovascular-function.shtml. URL: `https://commons.wikimedia.org/wiki/File:Sankey_diagram_human_circulatory_system.svg` (visited on 05/25/2016).

[7] David Gallagher, Audrey Adji, and Michael F O'Rourke. Validation of the transfer function technique for generating central from peripheral upper limb pressure waveform. *American journal of hypertension*, 17(11):1059–1067, 2004.

[8] Bernhard Hametner. Arterial pulse wave analysis - impact of models for impedance and wave reflection. PhD thesis. Institute of Analysis and Scientific Computing, Vienna University of Technology, 2011.

[9] Bernhard Hametner, Siegfried Wassertheurer, Johannes Kropf, et al. Oscillometric estimation of aortic pulse wave velocity: comparison with intra-aortic catheter measurements. *Blood pressure monitoring*, 18(3):173–176, 2013.

[10] Bernhard Hametner, Siegfried Wassertheurer, Johannes Kropf, et al. Wave reflection quantification based on pressure waveforms alone - methods, comparison, and clinical covariates. *Computer methods and programs in biomedicine*, 109(3):250–259, 2013.

[11] Abigael Heim, Lucas Liaudet, Bernard Waeber, et al. Pulse wave analysis of aortic pressure: diastole should also be considered. *Journal of hypertension*, 31(1):94–102, 2013.

[12] Annie Herbert, John Kennedy Cruickshank, Stéphane Laurent, et al. Establishing reference values for central blood pressure and its amplification in a general healthy population and according to cardiovascular risk factors. *European heart journal*, 35(44):3122–3133, 2014.

[13] Sarah A Hope, David B Tay, Ian T Meredith, et al. Waveform dispersion, not reflection, may be the major determinant of aortic pressure wave morphology. *American journal of physiology-heart and circulatory physiology*, 289(6):H2497–H2502, 2005.

[14] Alun D Hughes, Chloe Park, Justin Davies, et al. Limitations of augmentation index in the assessment of wave reflection in normotensive healthy individuals. *Plos one*, 8(3):e59371, 2013.

[15] Eugenijus Kaniusas. *Biomedical signals and sensors i: linking physiological phenomena and biosignals*. Springer Science & Business Media, 2012.

[16] Ari Lieber, Sandrine Millasseau, Laurent Bourhis, et al. Aortic wave reflection in women and men. *American journal of physiology-heart and circulatory physiology*, 299(1):H236–H242, 2010.

[17] Herbert Lippert. *Lehrbuch anatomie*. Urban & Fischer Verlag, 5th edition edition, 2000.

[18] Leonella Luzardo, Inés Lujambio, Mariana Sottolano, et al. 24-h ambulatory recording of aortic pulse wave velocity and central systolic augmentation: a feasibility study. *Hypertension research*, 35(10):980–987, 2012.

[19] Giuseppe Mancia, Robert Fagard, Krzysztof Narkiewicz, et al. 2013 esh/esc guidelines for the management of arterial hypertension - the task force for the management of arterial hypertension of the european society of hypertension (esh) and of the european society of cardiology (esc). *European heart journal*, 34:2159–2219, 2013.

[20] Giuseppe Mancia, Stefano Omboni, Gianfranco Parati, et al. Limited reproducibility of hourly blood pressure values obtained by ambulatory blood pressure monitoring: implications for studies on antihypertensive drugs. *Journal of hypertension*, 10(12):1531–1535, 1992.

[21] Carmel M McEniery, John R Cockcroft, Mary J Roman, et al. Central blood pressure: current evidence and clinical importance. *European heart journal*, 35(26):1719–1725, 2014.

[22] Gary F. Mitchell, Helen Parise, Emelia J. Benjamin, et al. Changes in arterial stiffness and wave reflection with advancing age in healthy men and women: the framingham heart study. *Hypertension*, 43:1239–1245, 2004.

[23] National Institutes of Health National Cancer Institute. Illustration of blood vessels including artery, arteriole, capillaries, vein and venule. URL: `https://commons.wikimedia.org/wiki/File:Capillaries.jpg` (visited on 05/31/2016).

[24] Wilmer Nichols, Michael O'Rourke, and Charalambos Vlachopoulos. *Mcdonald's blood flow in arteries. Theoretical, experimental, and clinical principles*. Hodder Arnold, 6th ed edition, 2011. ISBN: 9781444128789.

[25] David Nunan, Susannah Fleming, Bernhard Hametner, et al. Performance of pulse wave velocity measured using a brachial cuff in a community setting. *Blood pressure monitoring*, 19:315–319, 2014.

[26] David Nunan, Siegfried Wassertheurer, Daniel Lasserson, et al. Assessment of central haemomodynamics from a brachial cuff in a community setting. *Bmc cardiovascular disorders*, 12(1):1, 2012.

[27] Jens Nürnberger, Rene Michalski, Tobias R Türk, et al. Can arterial stiffness parameters be measured in the sitting position? *Hypertension research*, 34(2):202–208, 2011.

[28] Eoin O'Brien, Neil Atkins, George Stergiou, et al. European society of hypertension international protocol revision 2010 for the validation of blood pressure measuring devices in adults. *Blood pressure monitoring*, 15(1):23–38, 2010.

[29] Michael F O'Rourke and Alberto P Avolio. Arterial transfer functions: background, applications and reservations. *Journal of hypertension*, 26(1):8–10, 2008.

[30] Stephanie Parragh, Bernhard Hametner, Martin Bachler, et al. Non-invasive wave reflection quantification in patients with reduced ejection fraction. *Physiological measurement*, 36(2):179–190, 2015.

[31] Athanase D Protogerou, Antonis A Argyris, Theodoros G Papaioannou, et al. Left-ventricular hypertrophy is associated better with 24-h aortic pressure than 24-h brachial pressure in hypertensive patients: the safar study. *Journal of hypertension*, 32(9):1805–1814, 2014.

[32] Athanase D Protogerou, Harold Smulyan, and Michel E Safar. Closer to noninvasive out-of-office aortic blood pressure assessment a time to think and act. *Hypertension*, 58(5):765–767, 2011.

[33] Patrick Segers, Ernst Rietzschel, Steven Heireman, et al. Carotid tonometry versus synthesized aorta pressure waves for the estimation of central systolic blood pressure and augmentation index. *American journal of hypertension*, 18(9):1168–1173, 2005.

[34] James E Sharman, Richard Lim, Ahmad M Qasem, et al. Validation of a generalized transfer function to noninvasively derive central blood pressure during exercise. *Hypertension*, 47(6):1203–1208, 2006.

[35] Stefan Silbernagl and Rainer Klinke. *Lehrbuch der physiologie*. Thieme, 3rd edition edition, 2001.

[36] Harold Smulyan, Sylvain J Marchais, Bruno Pannier, et al. Influence of body height on pulsatile arterial hemodynamic data. *Journal of the american college of cardiology*, 31(5):1103–1109, 1998.

[37] Lee Stoner, James Faulkner, Andrew Lowe, et al. Should the augmentation index be normalized to heart rate? *Journal of atherosclerosis and thrombosis*, 21(1):11–16, 2014.

[38] Abigail Swillens and Patrick Segers. Assessment of arterial pressure wave reflection: methodological considerations. *Artery research*, 2(4):122–131, 2008.

[39] Yasuharu Tabara, Rieko Tachibana-Iimori, Miyuki Yamamoto, et al. Hypotension associated with prone body position: a possible overlooked postural hypotension. *Hypertension research*, 28(9):741–746, 2005.

[40] Anna Tahvanainen, Jenni Koskela, Antti Tikkakoski, et al. Analysis of cardiovascular responses to passive head-up tilt using continuous pulse wave analysis and impedance cardiography. *Scandinavian journal of clinical and laboratory investigation*, 69(1):128–137, 2009.

[41] Gerhard Thews, Ernst Mutschler, and Peter Vaupel. *Anatomie, physiologie, pathophysiologie des menschen*. Volume 6. Wissenschaftliche Verlagsgesellschaft, 2007.

[42] Alyssa A Torjesen, Na Wang, Martin G Larson, et al. Forward and backward wave morphology and central pressure augmentation in men and women in the framingham heart study. *Hypertension*, 64(2):259–265, 2014.

[43] LadyofHats (Mariana Ruiz - Villarreal). Simplified diagram of the human circulatory system in anterior view. 2009. URL: https://commons.wikimedia.org/wiki/File:Circulatory_System_en.svg (visited on 05/31/2016).

[44] Charalambos Vlachopoulos, Konstantinos Aznaouridis, Michael F O'Rourke, et al. Prediction of cardiovascular events and all-cause mortality with central haemodynamics: a systematic review and meta-analysis. *European heart journal*, 31(15):1865–1871, 2010.

[45] Wapcaplet and Yaddah. Diagram of the human heart. URL: https://commons.wikimedia.org/wiki/File:Diagram_of_the_human_heart_(cropped).svg (visited on 05/31/2016).

[46] S Wassertheurer, J Kropf, T Weber, et al. A new oscillometric method for pulse wave analysis: comparison with a common tonometric method. *Journal of human hypertension*, 24(8):498–504, 2010.

[47] Siegfried Wassertheurer, Christopher Mayer, and Felix Breitenecker. Modeling arterial and left ventricular coupling for non-invasive measurements. *Simulation modelling practice and theory*, 16(8):988–997, 2008.

[48] Thomas Weber, Marcus Ammer, Martin Rammer, et al. Noninvasive determination of carotid–femoral pulse wave velocity depends critically on assessment of travel distance: a comparison with invasive measurement. *Journal of hypertension*, 27(8):1624–1630, 2009.

[49] Thomas Weber, Bernhard Hametner, and Siegfried Wassertheurer. Travel distance estimation for carotid femoral pulse wave velocity: is the gold standard a real one? *Journal of hypertension*, 29(12):2491–2494, 2011.

[50] Thomas Weber, Siegfried Wassertheurer, Martin Rammer, et al. Validation of a brachial cuff-based method for estimating central systolic blood pressure. *Hypertension*, 58(5):825–832, 2011.

[51] Wolfgang Weisz, Markus Tölle, Walter Zidek, et al. Validation of the mobil-o-graph: 24 h-blood pressure measurement device. *Blood pressure monitoring*, 15(4):225–228, 2010.

[52] N Westerhof, Pk Sipkema, GC Van Den Bos, et al. Forward and backward waves in the arterial system. *Cardiovascular research*, 6(6):648–656, 1972.

[53] WHO, editor. Cardiovascular diseases, fact sheet nr 317. 2015. URL: `http://www.who.int/mediacentre/factsheets/fs317/en/` (visited on 05/20/2016).

[54] Ian B Wilkinson, Helen MacCallum, Laura Flint, et al. The influence of heart rate on augmentation index and central arterial pressure in humans. *The journal of physiology*, 525(1):263–270, 2000.

[55] Ian B Wilkinson, Carmel M McEniery, and John R Cockcroft. Central blood pressure estimation for the masses moves a step closer. *Journal of human hypertension*, 24(8):495–497, 2010.